

We are IntechOpen, the world's leading publisher of Open Access books Built by scientists, for scientists

6,900

Open access books available

186,000

International authors and editors

200M

Downloads

Our authors are among the

154

Countries delivered to

TOP 1%

most cited scientists

12.2%

Contributors from top 500 universities



WEB OF SCIENCE™

Selection of our books indexed in the Book Citation Index
in Web of Science™ Core Collection (BKCI)

Interested in publishing with us?
Contact book.department@intechopen.com

Numbers displayed above are based on latest data collected.
For more information visit www.intechopen.com



Microwave Heating in Moist Materials

Graham Brodie
The University of Melbourne
Australia

1. Introduction

The definition of “microwaves” is somewhat arbitrary; however microwaves are usually considered to be electromagnetic waves in the frequency range from 300 MHz to 300 GHz. Before World War II, there is little evidence of work on radio frequency or microwave heating; however Kassner (1937b) mentions industrial applications of microwave energy in two of his patents on spark-gap microwave generators (Kassner, 1937a, 1937b, 1938). Unfortunately early studies in radio frequency heating concluded that microwave heating of food stuffs would be most unlikely because the calculated electric field strength required to heat biological materials would approach the breakdown voltage of air (Shaw & Galvin, 1949).

A fortuitous discover by Spencer that microwave energy could heat food (Murray, 1958) lead to a series of patents (Spencer, 1947, 1949, 1952) and the development of microwave cooking equipment. The major advantages of microwave heating are its short start-up, precise control and volumetric heating (Ayappa et al., 1991); however microwave heating suffers from: uneven temperature distributions (Van Remmen et al., 1996; Brodie, 2008); unstable temperatures (Vriezinger, 1996, 1998, 1999; Vriezinger et al., 2002); and rapid moisture movement (Brodie, 2007b). This chapter will explore the theory and practice of microwave heating in moist materials.

2. Theory

Microwave heating is governed by Maxwell's electromagnetic equations:

$$\nabla \cdot \mathbf{E} = \frac{\rho_c}{\epsilon^*}, \quad \nabla \times \mathbf{E} = -\frac{\partial(\mu \mathbf{H})}{\partial t}, \quad \text{and} \quad \nabla \times \mathbf{H} = \mathbf{J}_c + \mathbf{J}_s + \frac{\partial(\epsilon^* \mathbf{E})}{\partial t} \quad (1)$$

From these, it is possible to derive a wave equation of the form:

$$\nabla^2 \mathbf{E} = \mu \left[\frac{\partial^2(\epsilon^* \mathbf{E})}{\partial t^2} + \frac{1}{2} \frac{\partial(\sigma_c \mathbf{E})}{\partial t} + \frac{\partial \mathcal{B}}{\partial t} \right] + \nabla \left(\frac{\rho_c}{\epsilon^*} \right) \quad (2)$$

Equation (2) is a forced, damped wave equation made up of three components:

- $\nabla^2 \mathbf{E} = \mu \left[\frac{\partial^2(\epsilon^* \mathbf{E})}{\partial t^2} + \frac{1}{2} \frac{\partial(\sigma_c \mathbf{E})}{\partial t} \right]$ is the damped wave response;

- $\mu \frac{\partial \mathbf{J}}{\partial t}$ accounts for any time varying current source embedded in the space of interest that creates the damped wave; and
- $\nabla \left(\frac{\rho_c}{\epsilon^*} \right)$ accounts for any static component to the field, associated with stationary charges embedded in the space of interest.

Assuming that all field sources lie outside the space occupied by the heated material and the incident microwave fields are monochromatic with an angular frequency ω , equation (2) simplifies to:

$$\nabla^2 \mathbf{E} + f^2 \mathbf{E} = 0 \quad (3)$$

Where:

$$f = \frac{\omega}{c} \sqrt{\kappa' \left[1 - j \frac{\left(\frac{2}{\omega} \frac{\partial \kappa'}{\partial t} + \kappa'' \right)}{\kappa'} \right] - \left(\frac{1}{\omega^2} \frac{\partial^2 \kappa'}{\partial t^2} + \frac{1}{\omega} \frac{\partial \kappa''}{\partial t} \right)} \quad (4)$$

Because the angular frequency ω is so large at microwave frequencies, equation (4) can be nicely approximated by:

$$f = \frac{\omega}{c} \sqrt{\kappa' \left[1 - j \frac{\kappa''}{\kappa'} \right]} \quad (5)$$

This can be rearranged to become:

$$f = \alpha + j\beta \quad (6)$$

Where:

$$\alpha = \frac{\omega}{c} \sqrt{\frac{\kappa'}{2} \left(\sqrt{1 + \left(\frac{\kappa''}{\kappa'} \right)^2} + 1 \right)} \quad (7)$$

and

$$\beta = \frac{\omega}{c} \sqrt{\frac{\kappa'}{2} \left(\sqrt{1 + \left(\frac{\kappa''}{\kappa'} \right)^2} - 1 \right)} \quad (8)$$

The form of the Laplacian operator (∇^2) in equation (3) depends entirely on the geometry of the problem.

2.1 Simultaneous heat and moisture movement

Any realistic analysis of microwave heating in moist materials must account for simultaneous heat and moisture diffusion through the material. The coupling between heat and moisture transfer is well known but not very well understood (Chu & Lee, 1993). Henry

(1948) first proposed the theory for diffusion of heat and moisture into a textile package. Crank (1979) presented a more thorough development of Henry’s work. This theory has been rewritten and used by many authors (Chu & Lee, 1993; Vos et al., 1994; Fan et al., 2000; Wang et al., 2002; Fan, 2004; Brodie, 2007b).

The amount of water vapour moving into a small section of porous material is the sum of any net increase in moisture content in the air space and the net increase in moisture content of the material's fibres (Crank, 1979). Therefore:

$$a_v \tau_v D_a \cdot \nabla^2 M_v = a_v \frac{\partial M_v}{\partial t} + (1 - a_v) \rho_s \frac{\partial M_s}{\partial t} \tag{9}$$

Heat is evolved because of microwave heating and moisture absorption by the material; therefore the thermal diffusion equation, which includes a volumetric heat source, is:

$$C\rho \frac{\partial T}{\partial t} = k\nabla^2 T + L\rho \frac{\partial M_s}{\partial t} + q \tag{10}$$

If a linear relationship between the moisture content of a material, the moisture vapour concentration in the air spaces in the material and the temperature is assumed (Henry, 1948; Crank, 1979), then:

$$\frac{\partial M_s}{\partial t} = \sigma \frac{\partial M_v}{\partial t} - \omega \frac{\partial T}{\partial t} \tag{11}$$

where σ and ω are constants of association between heat transfer and moisture vapour concentration. Substituting from equation (11) into equations (9) and (10) and combining the two equations yields:

$$\nabla^2 (pM_v + nT) - \frac{\partial}{\partial t} \left\{ \begin{aligned} & \left[\frac{1}{\tau_v D_a} \left(1 + \frac{(1 - a_v) \sigma \rho_s}{a_v} \right) - \frac{n \rho \sigma L}{pk} \right] pM_v + \\ & \left[\frac{C\rho}{k} \left(1 + \frac{\omega L}{C} \right) - \frac{p(1 - a_v) \omega \rho_s}{n \tau_v D_a a_v} \right] nT \end{aligned} \right\} + \frac{nq}{k} = 0 \tag{12}$$

This can be expressed in a simpler form if $\Omega = pM_v + nT$:

$$\nabla^2 \Omega - \frac{1}{\gamma} \frac{\partial \Omega}{\partial t} + \frac{nq}{k} = 0 \tag{13}$$

The constants of association, p and n, are calculated to satisfy:

$$\frac{1}{\gamma} = \left[\frac{1}{\tau_v D_a} \left(1 + \frac{(1 - a_v) \sigma \rho_s}{a_v} \right) - \frac{n \rho \sigma L}{pk} \right] = \left[\frac{C\rho}{k} \left(1 + \frac{\omega L}{C} \right) - \frac{p(1 - a_v) \omega \rho_s}{n \tau_v D_a a_v} \right] \tag{14}$$

Equation (14) implies that the combined heat and moisture diffusion coefficient (γ) has two independent values. This is consistent with Henry’s (1948) equation for simultaneous heat and moisture diffusion in textiles.

Henry (1948) showed that a change in external temperature or humidity (or both), “results in a coupled diffusion of moisture and heat”. Henry (1948) also states that “the diffusion constants

appropriate to these two quantities are always such that one is greater and the other less than either of the diffusion constants which would be observed for the moisture or heat, were these not coupled by the interaction”.

The slower diffusion coefficient of the coupled system is less than either the isothermal diffusion constant for moisture or the constant vapour concentration coefficient for heat diffusion, whichever is less, but never by more than one half (Henry, 1948). The faster diffusion coefficient is always many times greater than either of these independent diffusion constants (Henry, 1948).

Considerable evidence exists in literature for rapid heating and drying during microwave processing (Rozsa, 1995; Zielonka & Dolowy, 1998; Torgovnikov & Vinden, 2003); therefore it is reasonable to assume that the faster diffusion wave dominates microwave heating in moist materials. A slow heat and moisture diffusion wave should also exist; however observing this slow wave may be difficult and no evidence of its influence on microwave heating has been seen in literature so far.

2.2 Solutions to the microwave heating equation

Approximate solutions to equation (13) are sought under assumptions of uniform material properties for rectangular, cylindrical and spherical geometries. The aim is to readily identify the influence of geometry over microwave fields and temperature distributions. It is recognised that the derived equations will only provide approximate solutions to the diffusion problem, however the solutions are sufficiently accurate to provide some insight into the influence of geometry over temperature distributions during microwave heating.

2.3 Microwave heating in rectangular coordinates

Beginning with Maxwell's equations, Ayappa et al. (1991) demonstrate that the average power density ($W\ m^{-2}$) at a distance z below the irradiated surface of a material block of thickness W is:

$$q(z) = \omega \varepsilon_0 \kappa'' (\tau E)^2 \frac{\left\{ e^{-2\beta z} + 2\Gamma e^{-2\beta W} \cos[\delta + 2\alpha(W-z)] + \Gamma^2 e^{-2\beta W} e^{-2\beta(W-z)} \right\}}{2(1 - 2\Gamma^2 e^{-2\beta W} \cos(2\delta + 2\alpha W) + \Gamma^4 e^{-4\beta W})} \quad (15)$$

Where:

$$\delta = \tan^{-1} \left[\frac{2(\alpha_1 \beta_2 - \alpha_2 \beta_1)}{(\alpha_1^2 + \beta_1^2) - (\alpha_2^2 + \beta_2^2)} \right] \quad (16)$$

$$\Gamma = \frac{\sqrt{(\beta_1 - \beta_2)^2 + (\alpha_1 - \alpha_2)^2}}{\sqrt{(\beta_1 + \beta_2)^2 + (\alpha_1 + \alpha_2)^2}} \quad (17)$$

$$\tau = \frac{\sqrt{4(\alpha_1^2 + \beta_1^2)}}{\sqrt{(\beta_1 + \beta_2)^2 + (\alpha_1 + \alpha_2)^2}} \quad (18)$$

Provided the following boundary conditions are applied, solutions to equation (13) can be found using the Laplace transformation technique:

$$h\Omega \Big|_{\text{surface}} = -k \frac{\partial \Omega}{\partial z} \Big|_{\text{surface}} \quad (19a)$$

$$\frac{d\Omega}{dz} \Big|_{\text{centre}} = 0 \quad (19b)$$

$$\frac{d^2\Omega}{dz^2} \Big|_{\text{centre}} = 0 \quad (19c)$$

The Laplace transformation of equation (13) is:

$$\nabla^2 \Omega(s) - \frac{s}{\gamma} \Omega(s) + n\omega \varepsilon_0 \kappa''(\tau E)^2 \frac{\left\{ e^{-2\beta z} + 2\Gamma e^{-2\beta W} \cos[\delta + 2\alpha(W-z)] + \Gamma^2 e^{-2\beta W} e^{-2\beta(W-z)} \right\}}{2sk(1 - 2\Gamma^2 e^{-2\beta W} \cos(2\delta + 2\alpha W) + \Gamma^4 e^{-4\beta W})} = 0 \quad (20)$$

Solutions to equation (20) are found by combining the solution to the complementary function $\nabla^2 \Omega_o(s) - \frac{s}{\gamma} \Omega_o(s) = 0$ with any particular solutions to the full differential equation (Bowman, 1931).

Adopting rectangular coordinates and applying the limit theorem, i.e., $\lim_{t \rightarrow 0} f(t) = \lim_{s \rightarrow \infty} F(s)$, to ensure that the solution is bounded at time $t = 0$ yields:

$$\Omega(s) = A e^{-\sqrt{\frac{s}{\gamma}} z} + n\omega \varepsilon_0 \kappa''(\tau E)^2 \frac{\left\{ e^{-2\beta z} + 2\Gamma e^{-2\beta W} \cos[\delta + 2\alpha(W-z)] + \Gamma^2 e^{-2\beta W} e^{-2\beta(W-z)} \right\}}{2sk \left(\frac{s}{\gamma} - 4\beta^2 \right) (1 - 2\Gamma^2 e^{-2\beta W} \cos(2\delta + 2\alpha W) + \Gamma^4 e^{-4\beta W})} \quad (21)$$

This can now be solved using standard mathematical tables (Crank, 1979) to yield:

$$\Omega(t) = \frac{Az}{2\sqrt{\pi\gamma t^3}} e^{-\frac{z^2}{4\gamma t}} + n\omega \varepsilon_0 \kappa''(\tau E)^2 \left(e^{4\gamma\beta^2 t} - 1 \right) \frac{\left\{ e^{-2\beta z} + 2\Gamma e^{-2\beta W} \cos[\delta + 2\alpha(W-z)] + \Gamma^2 e^{-2\beta W} e^{-2\beta(W-z)} \right\}}{8k\beta^2 (1 - 2\Gamma^2 e^{-2\beta W} \cos(2\delta + 2\alpha W) + \Gamma^4 e^{-4\beta W})} \quad (22)$$

Applying the first boundary condition to evaluate A yields:

$$\Omega'(t) = \frac{n\omega \varepsilon_0 \kappa''(\tau E)^2 \left(e^{4\gamma\beta^2 t} - 1 \right)}{8k\beta^2 (1 - 2\Gamma^2 e^{-2\beta W} \cos(2\delta + 2\alpha W) + \Gamma^4 e^{-4\beta W})} (\Phi + \Psi + \Theta) + \Omega_o \quad (23)$$

where

$$\Phi = e^{-2\beta z} + \left(\frac{h}{k} + 2\beta \right) z e^{\frac{-z^2}{4\gamma t}} \quad (24)$$

$$\Psi = 2\Gamma e^{-2\beta W} \left\{ \cos[\delta + 2\alpha(W-z)] + \left[\frac{h}{k} \cos(\delta + 2\alpha W) - 2\alpha \sin(\delta + 2\alpha W) \right] z e^{\frac{-z^2}{4\gamma t}} \right\} \quad (25)$$

And

$$\Theta = \Gamma^2 e^{-4\beta W} \left\{ e^{-2\beta z} + \left[\frac{h}{k} + 2\beta \right] z e^{\frac{-z^2}{4\gamma t}} \right\} \quad (26)$$

The analysis used to obtain equation (23) assumed that the incoming electromagnetic wave has a constant phase. In a multi-mode oven, this scenario is unlikely because the load is usually placed on a rotating turntable, or mode stirrers are employed to perturb the microwave fields. The net result is that the phase (δ) of the incoming wave varies considerably during the heating process. For simplicity, it has been assumed that δ regularly cycles through 2π radians during the heating process. Therefore:

$$\Omega(t) = \int_0^{2\pi} \Omega'(t) \cdot d\delta \quad (27)$$

This renders $\Psi = 0$, allowing equation (23) to simplify to:

$$\Omega(t) = \left\{ \frac{n\omega\epsilon_0\kappa''(\tau\mathbf{E})^2 (e^{4\gamma\beta^2 t} - 1)}{8k\beta^2 (1 - 2\Gamma^2 e^{-2\beta W} \cos(2\delta + 2\alpha W) + \Gamma^4 e^{-4\beta W})} \right\} (\Phi + \Theta) + \Omega_o \quad (28)$$

If either β or W become sufficiently large or if there is no inner surface to reflect from (i.e., $\Gamma = 0$), equation (23) can be simplified to become:

$$\Omega(t) = \left\{ \frac{n\omega\epsilon_0\kappa''(\tau\mathbf{E})^2 (e^{4\gamma\beta^2 t} - 1)}{8k\beta^2 (1 - 2\Gamma^2 e^{-2\beta W} \cos(2\delta + 2\alpha W) + \Gamma^4 e^{-4\beta W})} \right\} \Phi + \Omega_o \quad (29)$$

Equations (23) and (29) predict that when a slab or block is heated in a microwave oven, subsurface heating occurs with the maximum temperature located slightly below the material surface. This agrees with information presented by Van Remmen et al., (1996) and Zielonka and Gierlik (1999). When the thickness of the material is small, the maximum temperature occurs in the center of the heated slab because the "subsurface" temperature peaks coincide with the center of the slab. However when the thickness of the material increased, two temperature peaks appear. This is a direct result of field attenuation inside the material. When the slab or block is fairly small, very little wave attenuation occurs; however, when the slab or block becomes much larger, the fields are significantly attenuated near the center of the object.

2.4 Microwave heating in cylindrical coordinates

Temperature profiles in small-diameter cylinders usually exhibit pronounced core heating (Ohlsson & Risman, 1978; Van Remmen et al., 1996); on the other hand, temperature profiles in large cylinders exhibit subsurface heating, with the peak temperature occurring slightly below the surface (Van Remmen et al., 1996). The same is also true when the microwave fields can not penetrate very far into the cylinder (Van Remmen et al., 1996).

The refractive index, at microwave frequencies, for many moist materials is very high (refractive index > 8). Therefore, by Snell's law, it is reasonable to assume that any wave propagates radially inside the cylinder irrespective of the incident angle of the external wave. It is also assumed that the microwave oven's turntable or mode stirrer ensures that the long-term illumination of the cylinder is uniform over all exposed surfaces. Therefore, in cylindrical coordinates, equation (3) becomes:

$$\frac{d^2 E}{dr^2} + \frac{1}{r} \frac{dE}{dr} + f^2 E = 0 \tag{30}$$

The solution to equation (30) has the general form:

$$E = A J_0(fr) + B Y_0(fr) \tag{31}$$

For E to be bounded at the center of the cylinder, B must be equal to zero, and therefore $E = A J_0(fr)$. Oliveira and Franca (2002) present the same solution for the electric field in a cylinder.

The Bessel function addition theorem is now applied to this complex field:

$$J_0(x + jy) = \sum_{m=-\infty}^{\infty} J_m(x) J_{o-m}(jy) = \sum_{m=-\infty}^{\infty} J_m(x) I_{o-m}(y) \tag{32}$$

When the complex argument is small, this simplifies to:

$$J_0(x + jy) \approx J_0(x) I_0(y) \tag{33}$$

Yousif and Melka (1997) further show that when the real part of the argument is small, as would be the case when heating relatively small cylindrical objects in domestic microwave ovens, $J_0(x + jy) \approx I_0(y) - jx[I_1(y)]$. Therefore, except near the central axis of the cylinder, the real component of the electric field has the form $E = A I_0(\beta r)$.

When the electric field in the cylinder is normalized to the field at the surface of the cylinder, equation (31) becomes:

$$E = \tau E_o \frac{I_0(\beta r)}{I_0(\beta r_o)} \tag{34}$$

Therefore, the heat and moisture diffusion equation in cylindrical coordinates is:

$$\frac{\partial^2 \Omega}{\partial r^2} + \frac{1}{r} \frac{\partial \Omega}{\partial r} - \frac{1}{\gamma} \frac{\partial \Omega}{\partial t} + \frac{n \omega \epsilon_o \kappa'' \tau^2 E_o^2}{k} \frac{I_0(2\beta r)}{I_0(2\beta r_o)} = 0 \tag{35}$$

Note: $[I_0(\beta r)]^2 \approx I_0(2\beta r)$.

Equation (35) can be solved using the Laplace transformation technique. It is customary to solve for the complementary (static) version of equations (35), by combining one or more solutions of $\frac{\partial^2 \Omega(s)}{\partial r^2} + \frac{1}{r} \frac{\partial \Omega(s)}{\partial r} - \frac{s}{\gamma} \Omega(s) = 0$ with a specific solution to the full equation. In

order to find a solution to the complementary function, a substitution of the form $z = \sqrt{\frac{s}{\gamma}}r$ is made. The complementary function then becomes a modified Bessel equation, which has the standard solution of the form:

$$\Omega_a(s) = AK_0(z) + BI_0(z) \quad (36)$$

Applying the limit theorem $\left[\lim_{t \rightarrow 0} f(t) = \lim_{s \rightarrow \infty} F(s) \right]$ to ensure that the solution is bounded at time $t = 0$ implies that $B = 0$.

In order to investigate what is happening near the surface of the heated cylinder, it is necessary to seek a particular solution to the complementary function. The most appropriate form of this solution would be: $\Omega_b(s) = e^{\lambda(r_0-r)}$. Substituting into the complementary function to evaluate λ , yields:

$$\Omega_b(s) = Ae^{\frac{1}{2r} + \sqrt{\frac{1}{4r^2} + \frac{s}{\gamma}}(r_0-r)} + Be^{\frac{1}{2r} - \sqrt{\frac{1}{4r^2} + \frac{s}{\gamma}}(r_0-r)} \quad (37)$$

Now γ is usually very small ($\approx 10^{-7}$), so except in the case when r is infinitesimally close to zero, equation (37) can be approximated by:

$$\Omega_b(s) = Ae^{\sqrt{\frac{s}{\gamma}}(r_0-r)} + Be^{-\sqrt{\frac{s}{\gamma}}(r_0-r)} \quad (38)$$

Again applying the limit theorem to keep the temperature bounded at time zero suggests that:

$$\Omega_b(s) = Be^{-\sqrt{\frac{s}{\gamma}}(r_0-r)} \quad (39)$$

A particular solution to equation (35) should be of the form $\Omega_c(s) = M \cdot I_0(2\beta r)$. Substituting into equation (35) and evaluating M yields:

$$\Omega_c(s) = \frac{n\omega\epsilon_0\kappa''\tau^2 E_0^2}{ks\left(\frac{s}{\gamma} - 4\beta^2\right)} \frac{I_0(2\beta r)}{I_0(2\beta r_0)} \quad (40)$$

Therefore, the combined solution becomes:

$$\Omega(s) = \Omega_a(s) + \Omega_b(s) + \Omega_c(s) \quad (41)$$

Or

$$\Omega(s) = AK_0\left(\sqrt{\frac{s}{\gamma}}r\right) + Be^{-\sqrt{\frac{s}{\gamma}}(r_0-r)} + \frac{n\omega\epsilon_0\kappa''\tau^2 E_0^2}{ks\left(\frac{s}{\gamma} - 4\beta^2\right)} \frac{I_0(2\beta r)}{I_0(2\beta r_0)} \quad (42)$$

This can be solved using standard mathematical tables (Crank, 1979) to yield:

$$\Omega(t) = \frac{A}{2t} e^{\frac{-r^2}{4\gamma t}} + \frac{B(r_o - r)}{2\sqrt{\pi\gamma t^3}} e^{\frac{-(r_o - r)^2}{4\gamma t}} + \frac{n\omega\varepsilon_o\kappa''\tau^2 E_o^2 (e^{4\beta^2\gamma t} - 1)}{4k\beta^2} \frac{I_o(2\beta r)}{I_o(2\beta r_o)} + \Omega_o \quad (43)$$

To evaluate the full temperature/ moisture distribution requires application of the following boundary conditions:

$$\left. \frac{d\Omega(t)}{dr} \right|_{r=0} = 0 \text{ and } -k \left. \frac{d\Omega(t)}{dr} \right|_{r=r_o} = h\Omega(t) \Big|_{r=r_o} \quad (44)$$

For the sake of simplifying the mathematics somewhat, the second boundary condition is applied to:

$$\Omega(t) = \frac{B(r_o - r)}{2\sqrt{\pi\gamma t^3}} e^{\frac{-(r_o - r)^2}{4\gamma t}} + \frac{n\omega\varepsilon_o\kappa''\tau^2 E_o^2 (e^{4\beta^2\gamma t} - 1)}{4k\beta^2} \frac{I_o(2\beta r)}{I_o(2\beta r_o)} \quad (45)$$

Because the approximation for the microwave power distribution used in equation (34) is not accurate near the center of the cylinder, the first boundary condition should be applied to:

$$\Omega(t) = \frac{A}{2t} e^{\frac{-r^2}{4\gamma t}} + \frac{n\omega\varepsilon_o\kappa''\tau^2 E_o^2 (e^{4\beta^2\gamma t} - 1)}{4k\beta^2} \frac{[J_o(\alpha r)I_o(\beta r)]^2}{[J_o(\alpha r_o)I_o(\beta r_o)]^2} \quad (46)$$

The analysis eventually yields:

$$\Omega(t) = \frac{n\omega\varepsilon_o\kappa''\tau^2 E_o^2 (e^{4\beta^2\gamma t} - 1)}{4k\beta^2 I_o(2\beta r_o)} (\Phi + \Psi + \Theta) + \Omega_o \quad (47)$$

In this case:

$$\Phi = \frac{4\alpha\gamma t}{[J_o(\alpha r_o)I_o(\beta r_o)]^2} e^{\frac{-r^2}{4\gamma t}} \quad (48)$$

$$\Psi = I_o(2\beta r) \quad (49)$$

And

$$\Theta = \left[2\beta I_1(2\beta r_o) + \frac{h}{k} I_o(2\beta r_o) \right] (r_o - r) e^{\frac{-(r_o - r)^2}{4\gamma t}} \quad (50)$$

2.5 Microwave heating in spherical coordinates

Spherical objects respond in a similar way to cylindrical objects in that small-diameter spheres usually exhibit pronounced core heating (Kritikos et al., 1981; Van Remmen et al.,

1996), while larger-diameter spheres or spheres made from very absorbent materials exhibit subsurface heating (Van Remmen et al., 1996). When spherical coordinates are applied, equation (3) becomes:

$$\frac{d^2 E}{dr^2} + \frac{2}{r} \frac{dE}{dr} + f^2 E = 0 \quad (51)$$

Following the same process as with the cylindrical analysis described above, the solution to equation (51) becomes:

$$E = \tau E_o \frac{j_o(fr)}{j_o(fr_o)} \quad (52)$$

Vriezinga (1998) presents an expression for the radial component of the spherical field in terms of ordinary Bessel functions:

$$E \propto A \sqrt{\frac{\pi}{2fr}} J_{n+(1/2)}(fr) \quad (53)$$

Now $\sqrt{\frac{\pi}{2fr}} J_{n+(1/2)}(fr) = j_n(fr)$; therefore, equation (52) is similar to the equation presented by Vriezinga. In the case of spherical coordinates, the heat/moisture diffusion equation becomes:

$$\frac{\partial^2 \Omega}{\partial r^2} + \frac{2}{r} \frac{\partial \Omega}{\partial r} - \frac{1}{\gamma} \frac{\partial \Omega}{\partial t} + \frac{n\omega \epsilon_o \kappa'' \tau^2 E_o^2}{k} \left[\frac{j_o(fr)}{j_o(fr_o)} \right]^2 = 0 \quad (54)$$

Following a similar derivation to the cylindrical case, the temperature/moisture distribution in spherical objects is eventually described by:

$$\Omega(t) = \frac{n\omega \epsilon_o \kappa'' \tau^2 E_o^2 (e^{4\beta^2 \gamma t} - 1)}{k\beta \cdot i_o(2\beta r_o)} (\Phi + \Psi + \Theta) + \Omega_o \quad (55)$$

In this case:

$$\Phi = \frac{\alpha \gamma t}{\beta [j_o(\alpha r_o) i_o(\beta r_o)]^2} e^{\frac{-r^2}{4\gamma t}} \quad (56)$$

$$\Psi = \frac{i_o(2\beta r)}{4\beta} \quad (57)$$

And

$$\Theta = \left[2\beta \cdot i_1(2\beta r_o) + \frac{h}{k} i_o(2\beta r_o) \right] \frac{(r_o - r)}{4\beta} e^{\frac{-(r_o - r)^2}{4\gamma t}} \quad (58)$$

Because cylinders and spheres tend to focus the microwave energy into the center of the workload, there is a stronger tendency towards core heating than in the rectangular slab. However, as the radius of the cylinder or sphere increases, the attenuation of the microwave fields becomes more pronounced, and there is a shift from predominantly core heating to predominantly subsurface heating. This phenomenon is well documented (Ohlsson & Risman, 1978; Kritikos et al., 1981; Van Remmen et al., 1996; Romano et al., 2005).

Even when the radius of the cylinder or sphere is fairly small, if the dielectric loss factor increases, there is a transition from predominantly core heating at lower loss factors to predominantly subsurface heating at higher loss factors. This was also observed by Van Remmen et al. (1996).

2.6 Multi-dimensional solutions

So far, this analysis has only considered single-dimensional heat transfer. Most real problems are multi-dimensional. The solution to multi-dimensional partial differential equations is a simple product of the single-dimensional solutions (Crank, 1979; Van Remmen et al., 1996). For example, the temperature distribution within a rectangular block, irradiated equally on all six faces, can be found by multiplying the temperature profiles associated with three slabs of thickness equal to the length, width, and height of the rectangular block.

Fig. 1 (a) shows the predicted temperature distribution in a rectangular block of agar gel heated in a multi-mode microwave oven. This distribution agrees with thermal images and other data found in the literature (Van Remmen et al., 1996; Zielonka & Gierlik, 1999). Agar gel is a useful medium for identifying hot spots during microwave heating because it melts at the hot spots, but remains solid where the temperature of the object is lower than its melting temperature. The theoretical temperature distributions in the agar gel block compare very well with the melting patterns in a block of agar gel (Fig. 1 (b)).

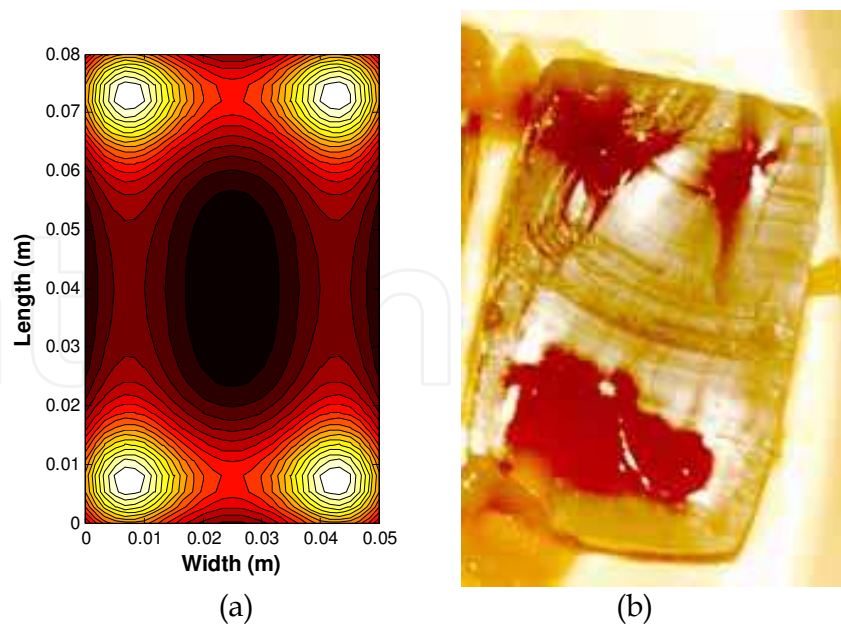


Fig. 1. (a) Theoretical multi-dimensional temperature distribution in a $50 \times 50 \times 80$ mm rectangular block of agar gel heated for 90 seconds (lighter colours represent hottest places) compared to (b) the actual melting patterns in a rectangular block of agar gel heated for 90 seconds in a domestic microwave oven.

The temperature distribution within a cylinder, which is irradiated equally on all surfaces, can be found by multiplying the radial temperature profile for the cylinder by the temperature profile associated with a slab of thickness equal to the height of the cylinder. When the cylinder's radius and loss factor are small, the temperature distribution resembles a "dumbbell" with two temperature peaks along the longitudinal axis, as shown in fig. 2a.

As the loss factor of the cylinder increases, the temperature profile is transformed such that there is an annulus of high temperature below the upper and lower circular surfaces, as shown in Fig. 3b. The same is true when the outer radius of the cylinder increases, as shown in Fig. 3c. The predicted temperature profiles shown in Fig. 3a and 3b are directly comparable with thermal images for cylindrical objects presented by Van Remmen et al. (1996).

The temperature distribution within a sphere irradiated equally on all surfaces is purely radial. Fig. 4 shows the temperature distributions in spheres of various diameters and loss factors. Again, these predicted temperature profiles are directly comparable with thermal images for spherical objects presented by Van Remmen et al. (1996).

3. The effect of heating time on temperature and drying

As would be expected, increasing microwave heating time increases the temperature in moist objects (Fig. 5). However, the relationship between time and temperature at a particular location inside the heated material is often non-linear because of the complexity of synchronized heat and moisture diffusion, changes of the spatial distribution of heat with time, partial drying of the material and their combined effect on the absorption of microwave energy.

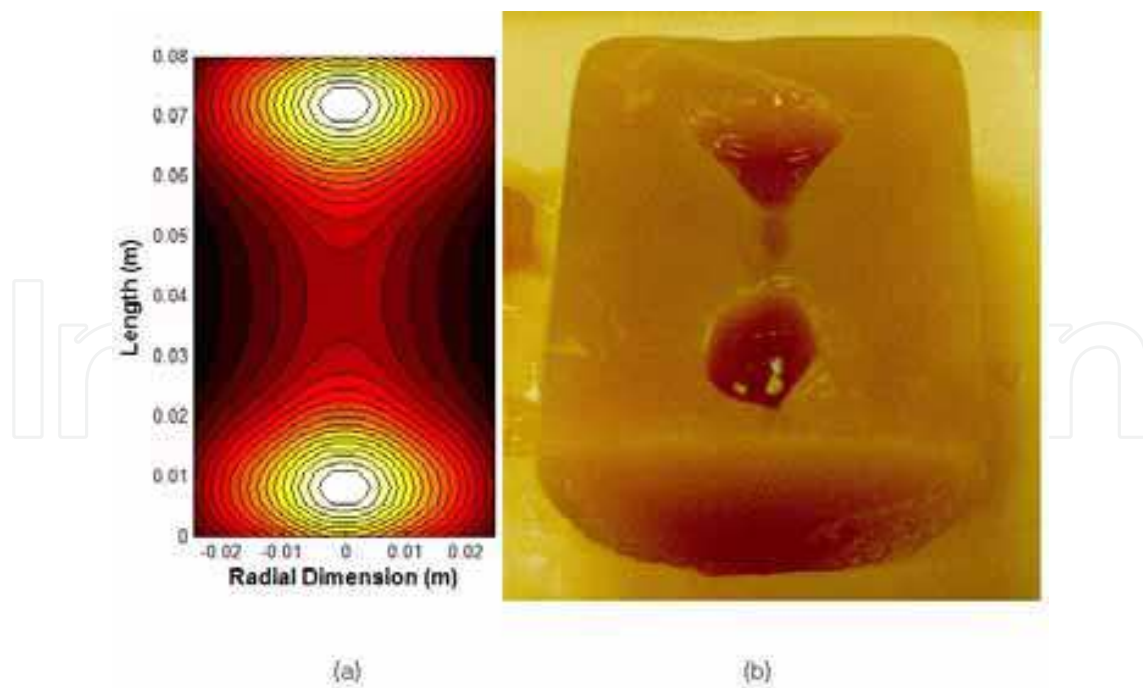


Fig. 2. (a) Theoretical multi-dimensional temperature distribution in a 50 mm diameter \times 80 mm long cylinder of agar gel compared to (b) the actual melting patterns in a cylinder of agar gel heated for 90 seconds in a domestic microwave oven.

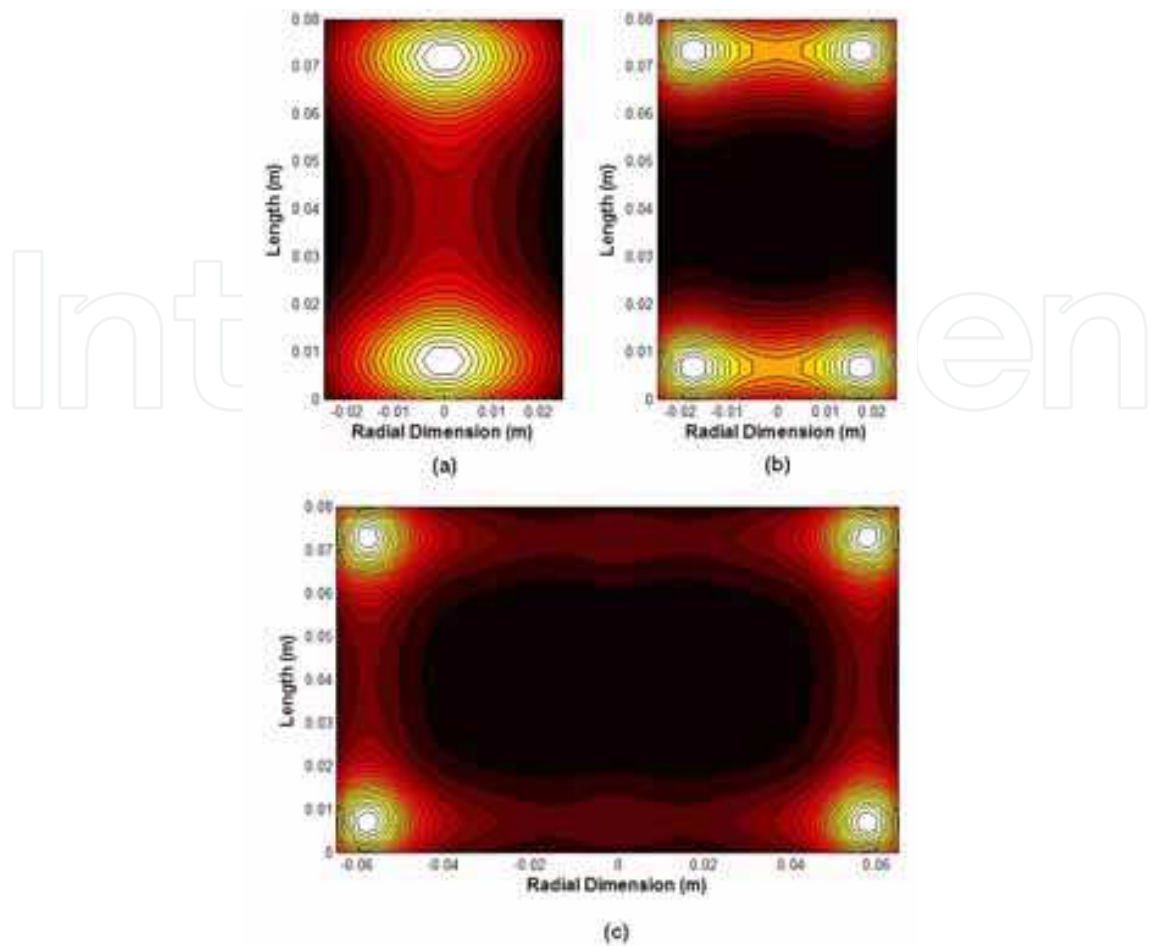


Fig. 3. Multi-dimensional temperature distribution along the longitudinal axis of 80 mm tall agar gel cylinders after 90 seconds of microwave heating for (a) radius = 25 mm, $\kappa' = 76.0$, $\kappa'' = 6.0$; (b) radius = 25 mm, $\kappa' = 76.0$, $\kappa'' = 15$; and (c) radius = 65 mm, $\kappa' = 76.0$, $\kappa'' = 6.0$ (lighter colours represent hottest places).

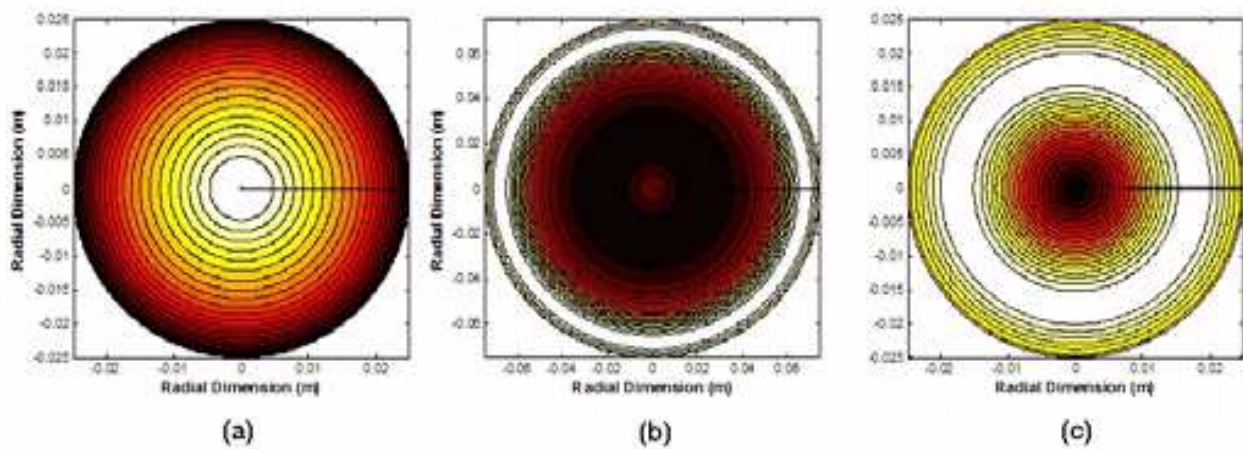


Fig. 4. Multi-dimensional temperature distribution in agar gel spheres after 90 seconds of microwave heating for (a) radius = 25 mm, $\kappa' = 76.0$, $\kappa'' = 10.0$; (b) radius = 75 mm, $\kappa' = 76.0$, $\kappa'' = 10.0$; and (c) radius = 25 mm, $\kappa' = 76.0$, $\kappa'' = 20.0$ (lighter colours represent hottest places).

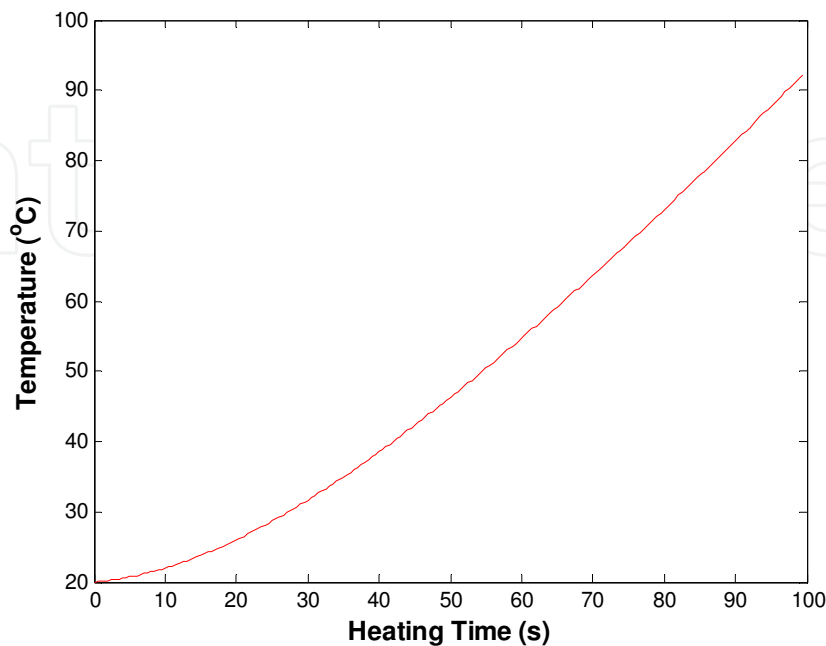


Fig. 5. Predicted temperature in the core of a 12 mm diameter cylinder of a generic plant material, initially having a moisture content of 80 % by weight, as a function of microwave heating time

Heating time not only affects the magnitude of the temperature but also the spatial distribution of heat. Fig. 6 shows a heating sequence for a rectangular block, while Fig. 7 shows the heating sequence for a cylinder. The change in temperature distribution as heating time increases is due to internal thermal diffusion from the zones where the microwave energy is being absorbed by the material to the rest of the object.

As may also be expected, microwave heating also dries moist materials. Conventional drying usually consists of a short constant rate drying period, where the rate of drying is controlled by surface evaporation, followed by a prolonged falling rate drying period (Fig. 8 a) during which the slow movement of moisture out of the object is controlled by the moisture diffusion properties of the material (Youngman et al., 1999). However, after a relatively short heat up period, microwave drying is usually quite linear with time (Fig. 8 b). This is because of the strong coupling between heat and moisture movement through the material. Therefore the rate of microwave drying is not limited by the internal diffusion properties of the material, but by the rate at which moisture can be evaporated from the surface of the material.

As the material dries, its dielectric properties will change significantly. These changes are too slow to affect the behaviour of individual cycles of the microwave fields; however they do affect microwave heating on the much longer thermal time scale.

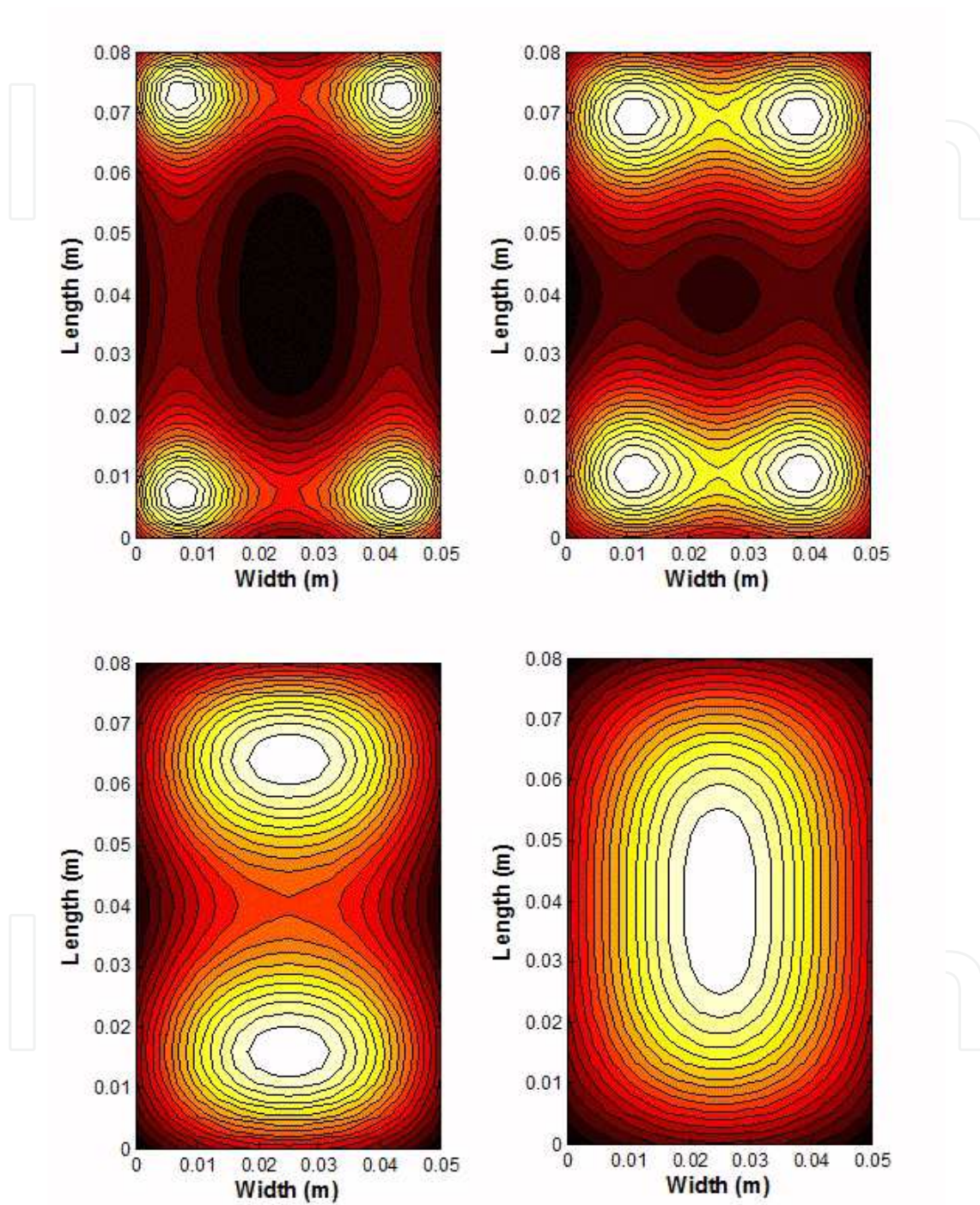


Fig. 6. Heating sequence for a $50 \times 50 \times 80$ mm rectangular block of agar gel heated for (left to right, top to bottom) 90, 190, 400 and 800 seconds in a multi-mode microwave oven.

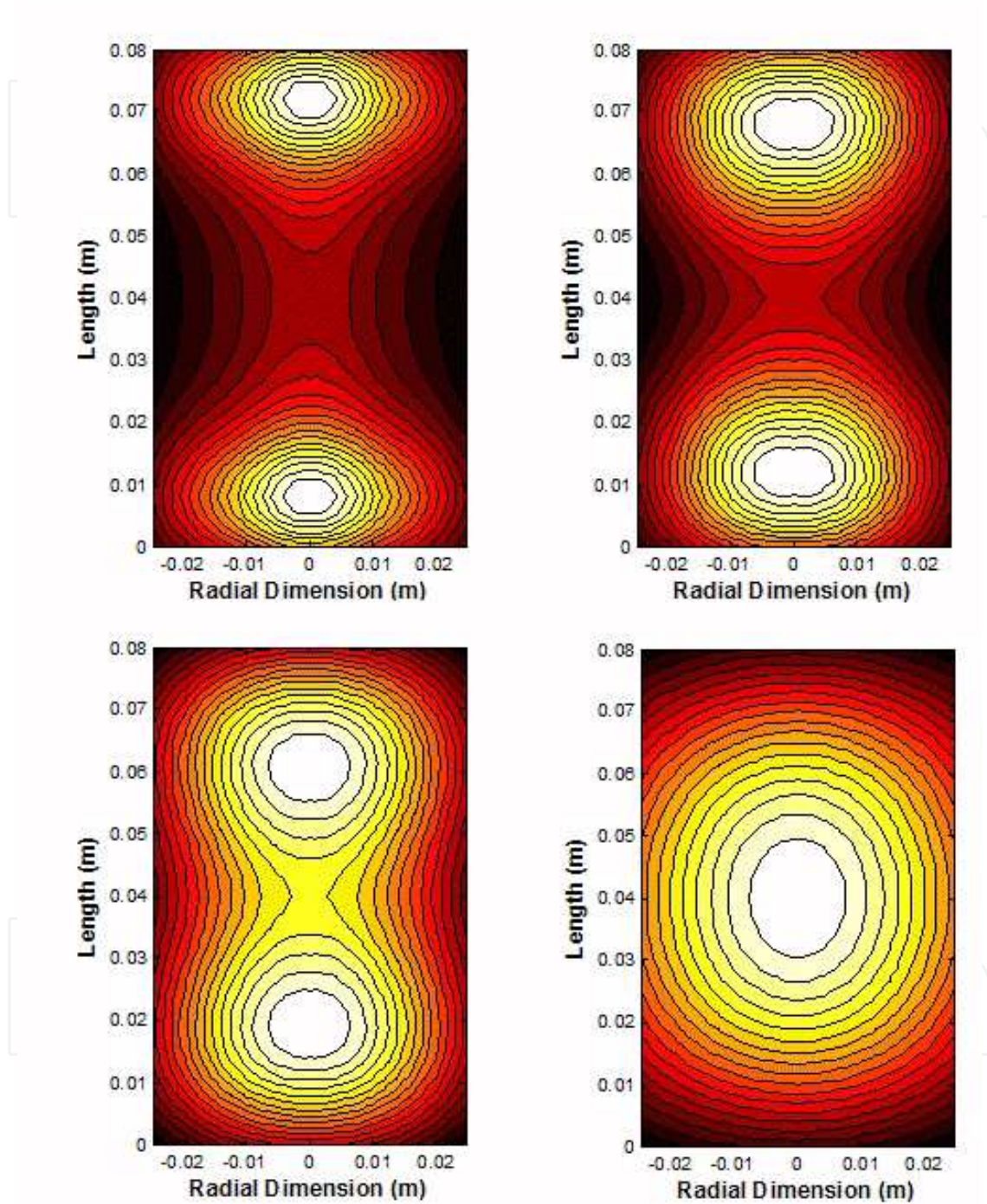


Fig. 7. Heating sequence for a 80 mm long \times 50 mm diameter cylinder of agar gel heated for (left to right, top to bottom) 90, 190, 400 and 800 seconds in a multi-mode microwave oven.

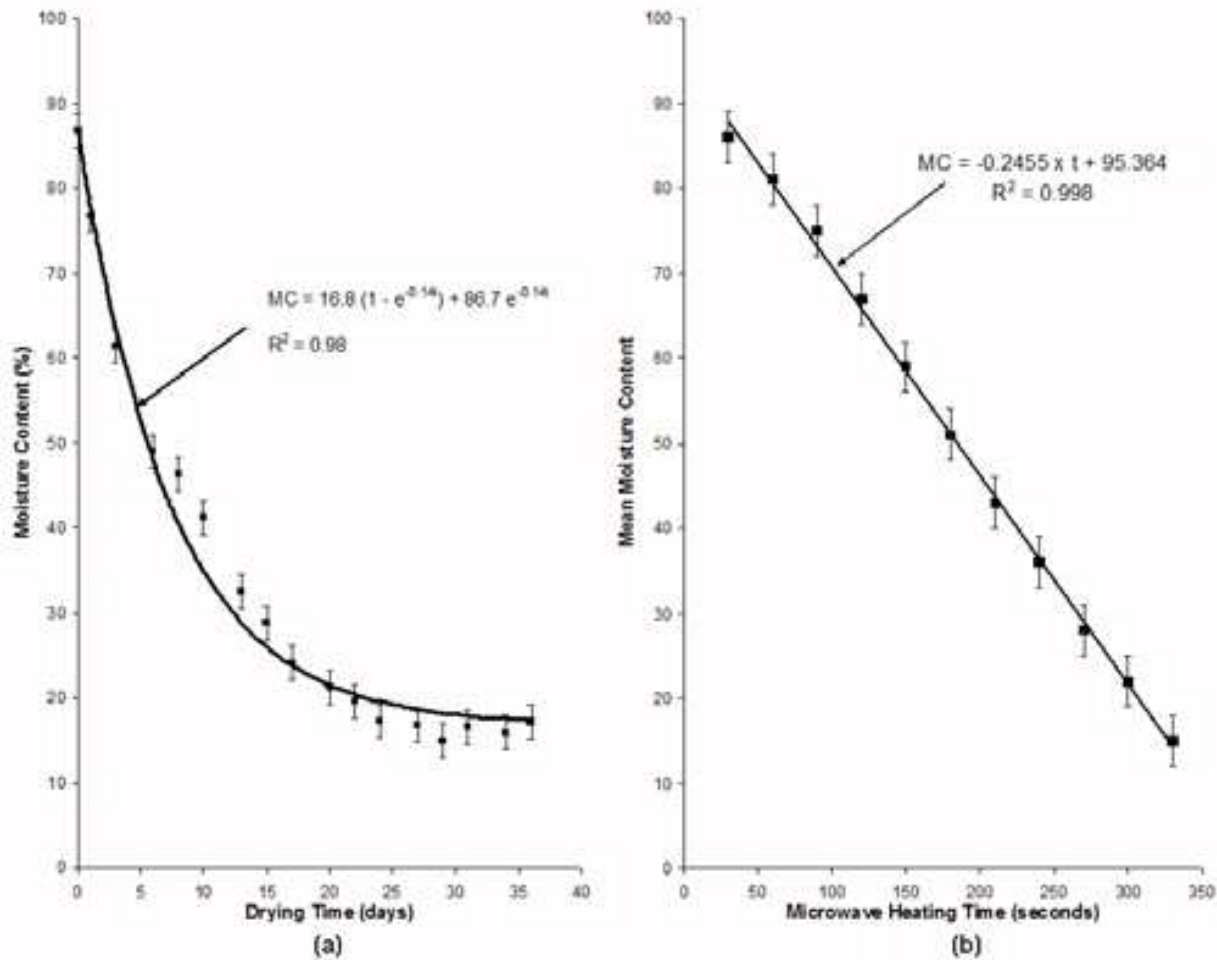


Fig. 8. Mean moisture content for 85 mm by 35 mm by 100 mm *Populus alba* wood samples (a) dried using conventional systems compared with (b) microwave drying.

4. The effect of changing dielectric properties on microwave heating

As an example of how the dielectric properties of moist materials change with moisture content, Ulaby and El-Rayes (1987) studied the dielectric properties of various plant materials at microwave frequencies. They determined that the dielectric behaviour of plant materials can be modeled using a Debye-Cole dual-dispersion dielectric model. Their model accounts for bound and free water in the plant material. Their equation for the dielectric constant of plant materials is:

$$\epsilon = \epsilon_s + v_{fw} \left(4.9 + \frac{73.5}{1 + j \frac{\omega}{123.78 \times 10^9}} - j \frac{113.1 \times 10^9 \times \sigma_c}{\omega} \right) + v_b \left(2.9 + \frac{55.0}{1 + \sqrt{j \frac{\omega}{1.13 \times 10^9}}} \right) \quad (59)$$

where

$$\epsilon_s = 1.7 - 0.74M_s + 6.16M_s^2 \quad (60)$$

$$v_{fw} = M_s(0.55M_s - 0.076) \quad (61)$$

$$v_b = \frac{1.5306M_s - 2.5909M_s^2 + 1.4355M_s^3}{1 - 0.60M_s} \quad (62)$$

and

$$\sigma_c = 1.27 \quad (63)$$

Plant material with high moisture content have higher dielectric constants (Fig. 9) and will therefore interact more with microwave fields.

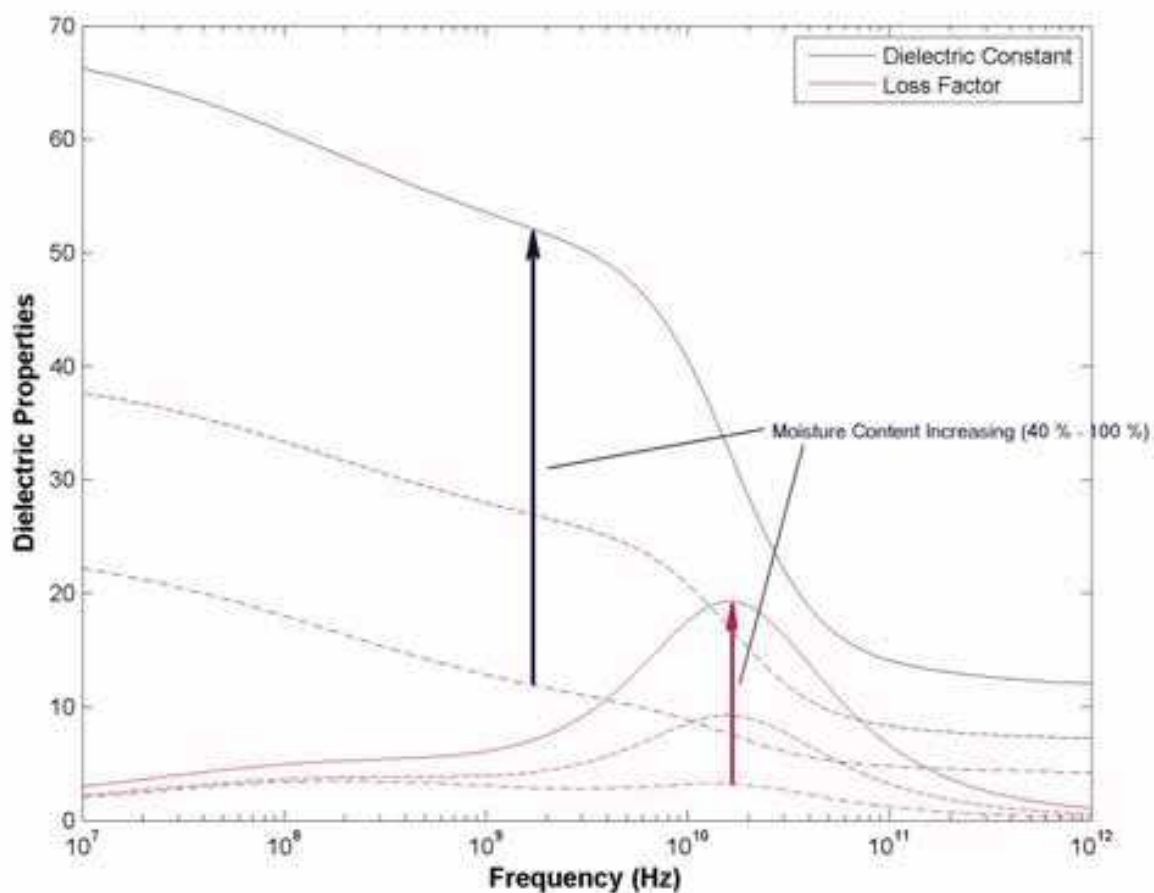


Fig. 9. Dielectric properties of plant materials as a function of frequency and moisture content.

It has also been well documented that the dielectric properties of most other materials are temperature and moisture dependent (Hill & Marchant, 1996; Vriezinger, 1998; Nelson et al., 2001). In order to explore what can happen when a material dries out during microwave heating, a semi-analytical technique can be used to analyse the microwave heating problem. As an example, the heating in a cylinder of plant material will be considered:

Equation (47) was used in an iterative calculation, where the temperature and moisture content of a plant based material was calculated after 0.5 second of microwave heating. This new temperature and moisture content was used to calculate the dielectric properties of the material using equation (59). These new dielectric properties were then used to calculate the next rise in temperature after another 0.5 seconds of microwave heating and so on. Moisture loss was assumed to have a linear relationship with microwave heating time as shown in Fig. 8 b. The results of this process are presented in Fig. 10.

The heating rate for 10 mm and 12 mm diameter cylinders is relatively constant with time; however there is a sudden temperature jump in the 15 mm diameter case when there is no change in the applied microwave power (Fig. 10). This sudden jump in temperature is the result of “*thermal runaway*”. Thermal runaway often destroys or chars the treated material, as seen in Fig. 11.

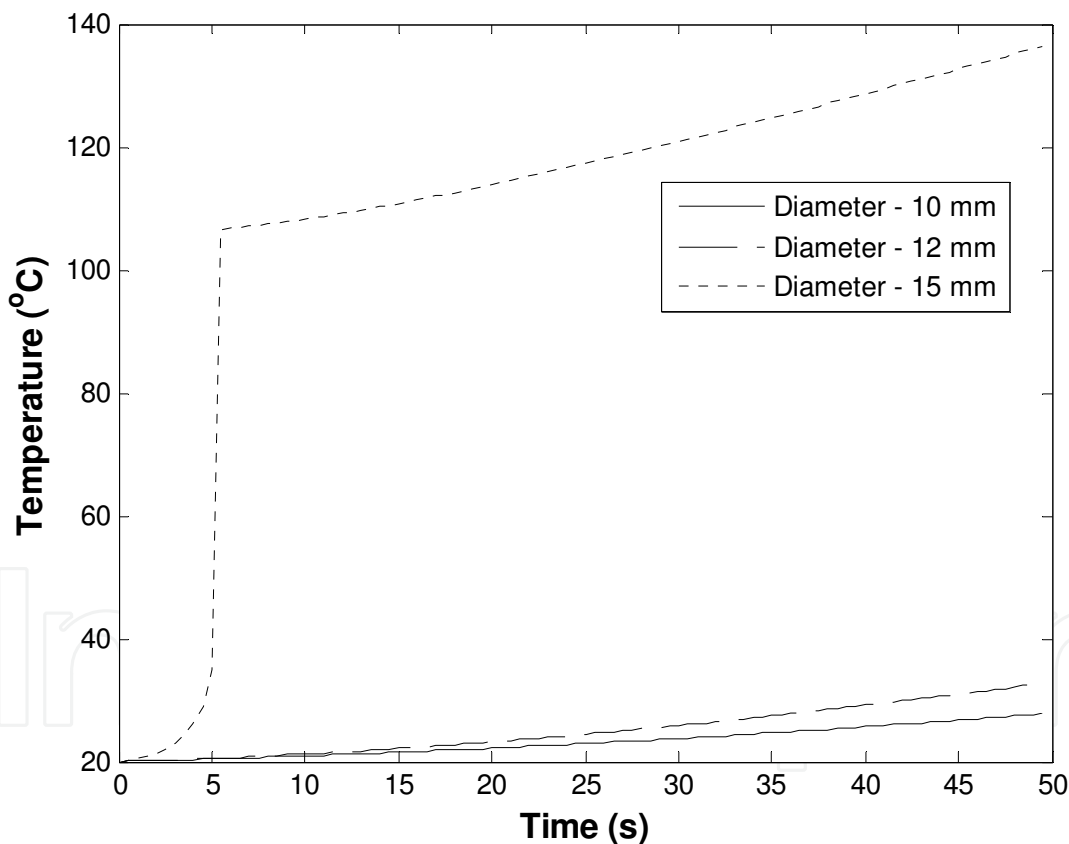


Fig. 10. Temperature response, at constant microwave power density, in the centre of a cylinder of plant based material, as a function of plant stem diameter, calculated using equation (47) and assuming constant moisture loss from a moisture content of 0.87 to 0.10 during microwave heating



Fig. 11. Charring, due to thermal runaway, in the core of a wood sample that was being dried in a microwave oven (Note: the location of the charring in comparison with the last image in Fig. 7)

4.1 Thermal runaway

Several authors (Vriezinger, 1998; Liu & Marchant, 2002) have suggested that the relationship between the applied microwave field strength and temperature follows a characteristic “S” shaped curve (Fig. 12).

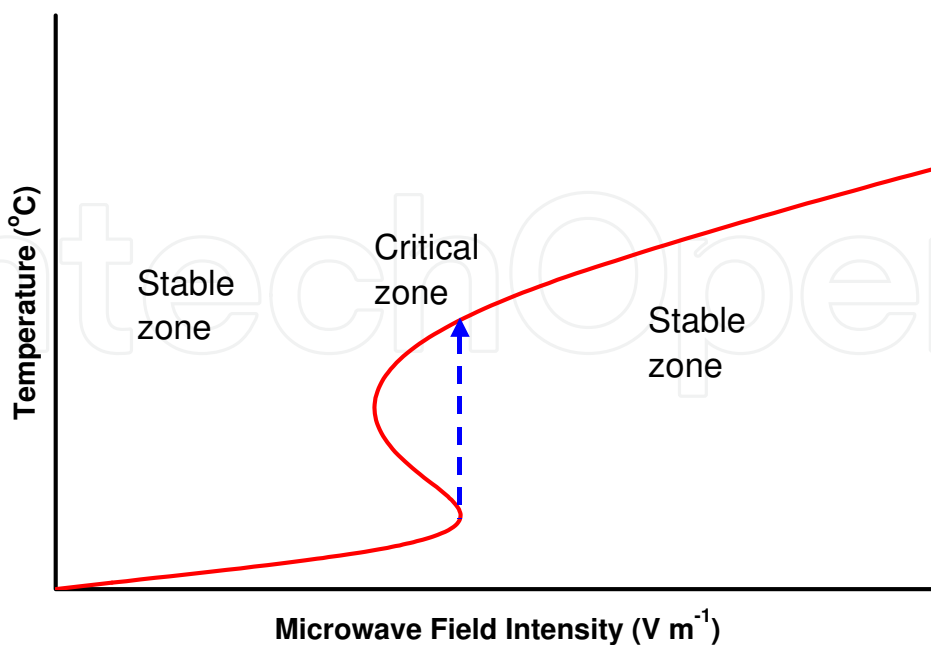


Fig. 12. The characteristic “S” shaped curve relating microwave field intensity and temperature

As microwave power is steadily increased, temperature rises steadily along the stable lower arm of the power curve shown in Fig. 12. In the critical power range, a small increase in electric field strength may shift the equilibrium temperature from the lower limb of the temperature curve to the higher limb, as indicated by the arrow in Fig. 12. The resulting change in temperature could be quite substantial and very rapid. This temperature jump gives rise to the potentially catastrophic phenomenon known as thermal runaway (Vriezina, 1998).

Thermal runaway is predicted by equations (23), (48) and (56). In each case, under the right combination of physical dimensions and dielectric properties of the material, the denominators of these equations can become very small thus forcing the temperature to become very large.

Thermal runaway manifests itself as a sudden jump in temperature over a very short time. It is linked to the temperature and moisture dependence of the material's dielectric properties. In some cases this can result in the material absorbing more microwave energy as it is heated, which in turn leads to faster heating which in turn leads to more energy absorption, etc. The net result is a sudden and uncontrolled jump in temperature, depending on the strength of the electromagnetic fields and the heating time.

The transfer of microwave energy into a material depends on the transmission coefficient of the material's surface, which also depends on the dielectric properties of the material. In many moist materials, the dielectric constant decreases with temperature and moisture loss (Vriezina, 1998). As the dielectric properties decrease with microwave heating, more energy enters the material due to increased transmission across the material's surface. This leads to faster heating, which leads to more energy transfer and so on.

Thermal runaway can also be caused by resonance (Vriezina, 1999) of the electromagnetic waves inside the object. As dielectric properties decrease with increasing temperature and moisture loss, the wavelength inside the material will increase in length. At a certain temperature and moisture, the electromagnetic wave will fit exactly within the dimensions of the heated object, causing resonance (Vriezina, 1999). Exactly at that moment the temperature will suddenly rise. Because heating and drying rates are dependent on the microwave field intensity, thermal runaway is strongly dependent on the intensity of the microwave's electric field strength (Fig. 13).

4.2 Examples of using thermal runaway in industrial microwave processes

In most cases, thermal runaway is a problem because it usually leads to destruction of the material (Zielonka et al., 1997); however it has been very effectively used in some applications:

Jerby et al. (2002) have developed a microwave drill that can drill holes through glass and ceramics by super-heating a very small section of the material using microwave induced thermal runaway. The system works by creating very intense microwave fields immediately in front of a needle like probe that extends into the material as the drilling process proceeds.

Vinden and Torgovnikov (2000) have also shown that the controlled application of intense microwave fields to green timber can rapidly boil free water inside the wood cells (Vinden & Torgovnikov, 2000; Ximing et al., 2002) causing microscopic fractures in the wood cells. When exposure to these intense fields is carefully managed, there is very little change in the visible appearance or strength of the wood; however there is a substantial change in wood density.

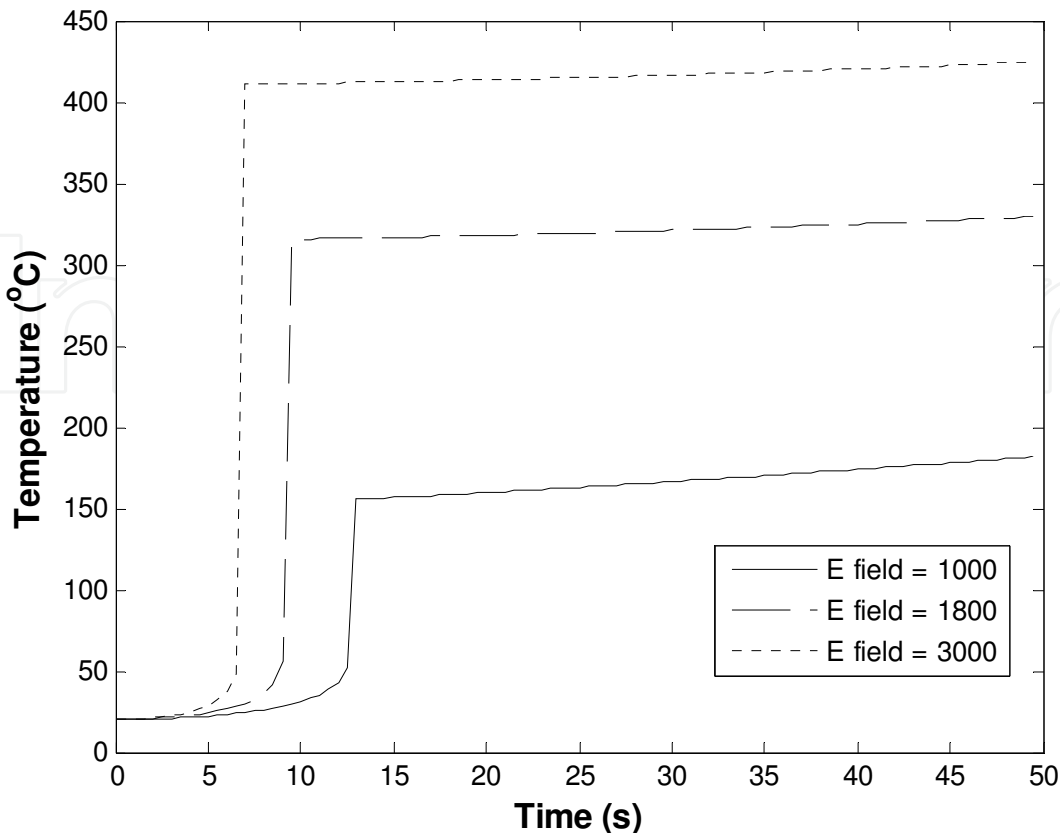


Fig. 13. Theoretical influence of microwave field strength over thermal runaway in a cylinder of plant based material of 16 mm diameter

Lawrence (2006) has demonstrated that this process can reduce the density of *Eucalyptus obliqua* wood by up to 12 %, as the wood cells are ruptured and the cross section of the wood is expanded due to internal steam explosions. This has been confirmed by other experimental work (Brodie, 2005, 2007a). This reduction in wood density leads to rapid drying in conventional systems with little loss in wood strength or quality. Microwave induced cell rupture has been linked to thermal runaway (Brodie, 2007a) in the timber.

5. Determining the electric field strength

The magnitude of the temperature/ moisture vapour wave and the onset of phenomenon such as thermal runaway depend on the electric field strength at the surface of the heated object; therefore it is important to model the field strength in the immediate vicinity of the heated object. Analytical solutions to Maxwell's equations can be found for simple microwave applicators, especially when they are empty (Meredith, 1994); however modeling of the microwave field strength in a loaded applicator requires the solution of Maxwell's equations in three dimensions when complex boundary conditions are imposed onto the system. It is almost impossible to determine these fields using analytical techniques.

Several techniques can be employed to simulate microwave fields in complex systems, including numerical techniques such as the Finite Difference Time Domain (FDTD) technique, proposed by Yee (1966). The FDTD method is a simple and elegant way to transform the differential form of Maxwell's equations from equation (1) into difference equations. Yee used an electric field grid (Fig. 14), which was offset both spatially and

temporally from a magnetic field grid to calculate the present field distribution throughout the computational domain in terms of the past field distribution.

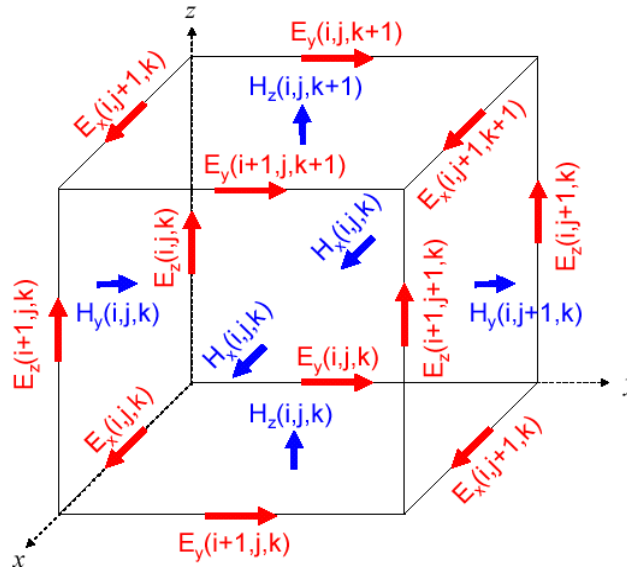


Fig. 14. Heating Single cell from the computational space used to compute Maxwell’s equations using FDTD techniques

Two of Maxwell’s equations can be transformed into difference equations for use in the FDTD algorithm:

$$E_x^{n+1}(i, j, k) = E_x^n(i, j, k) + \frac{\Delta t}{\epsilon} \left[\frac{H_z^{n+1/2}(i, j+1, k) - H_z^{n+1/2}(i, j, k)}{\Delta y} - \frac{H_y^{n+1/2}(i, j, k+1) - H_y^{n+1/2}(i, j, k)}{\Delta z} \right] \quad (64)$$

And

$$H_x^{n+1/2}(i, j, k) = H_x^{n-1/2}(i, j, k) + \frac{\Delta t}{\mu} \left[\frac{E_y^n(i, j, k+1) - E_y^n(i, j, k)}{\Delta z} - \frac{E_z^n(i, j+1, k) - E_z^n(i, j, k)}{\Delta y} \right] \quad (65)$$

Equations (64) and (65) calculate the electric and magnetic fields in the x direction. Similar equations are required to calculate E_y , E_z , H_y and H_z . These equations are used in a leap-frog scheme to incrementally march the electric and magnetic fields forward in time; therefore this numerical technique is a simulation of the microwave field rather than a direct solution of the field equations in space and time.

The FDTD method was originally developed to solve electromagnetic transmission problems associated with the communications industry (Kopyt et al., 2003), but it is now commonly used to determine electromagnetic field distributions within industrial microwave applicators (Kopyt et al., 2003). Numerical simulations of the microwave fields can provide valuable insight into the behaviour of microwave heating systems.

5.1 Strengths of the FDTD method

Every modeling technique has some strengths and some weaknesses. FDTD is a very versatile modeling technique. It is fairly intuitive, so users can easily understand what to expect from a given model.

FDTD is a time domain technique, and when a time-domain pulse (such as a Gaussian pulse) is used as an input to the computational model, a wide frequency range can be explored in a single simulation. This is extremely useful in applications where resonant frequencies are not known or when broadband performance is desirable.

Since FDTD is a time-domain technique which finds the E/H fields everywhere in the computational domain, it lends itself to providing animation displays (movies) of the E/H field movement throughout the model. FDTD also allows the user to specify the material properties at all points within the computational domain, which provides useful insight into the field distributions inside dielectric materials as they are processed using microwave systems. For example, when the FDTD technique is applied to a domestic microwave oven cavity in which various sized samples of water are included in the simulation space, it becomes clear that the microwave fields are significantly attenuated as the dimensions of the water sample increase (Fig. 15). This is because the water sample reduces the quality factor

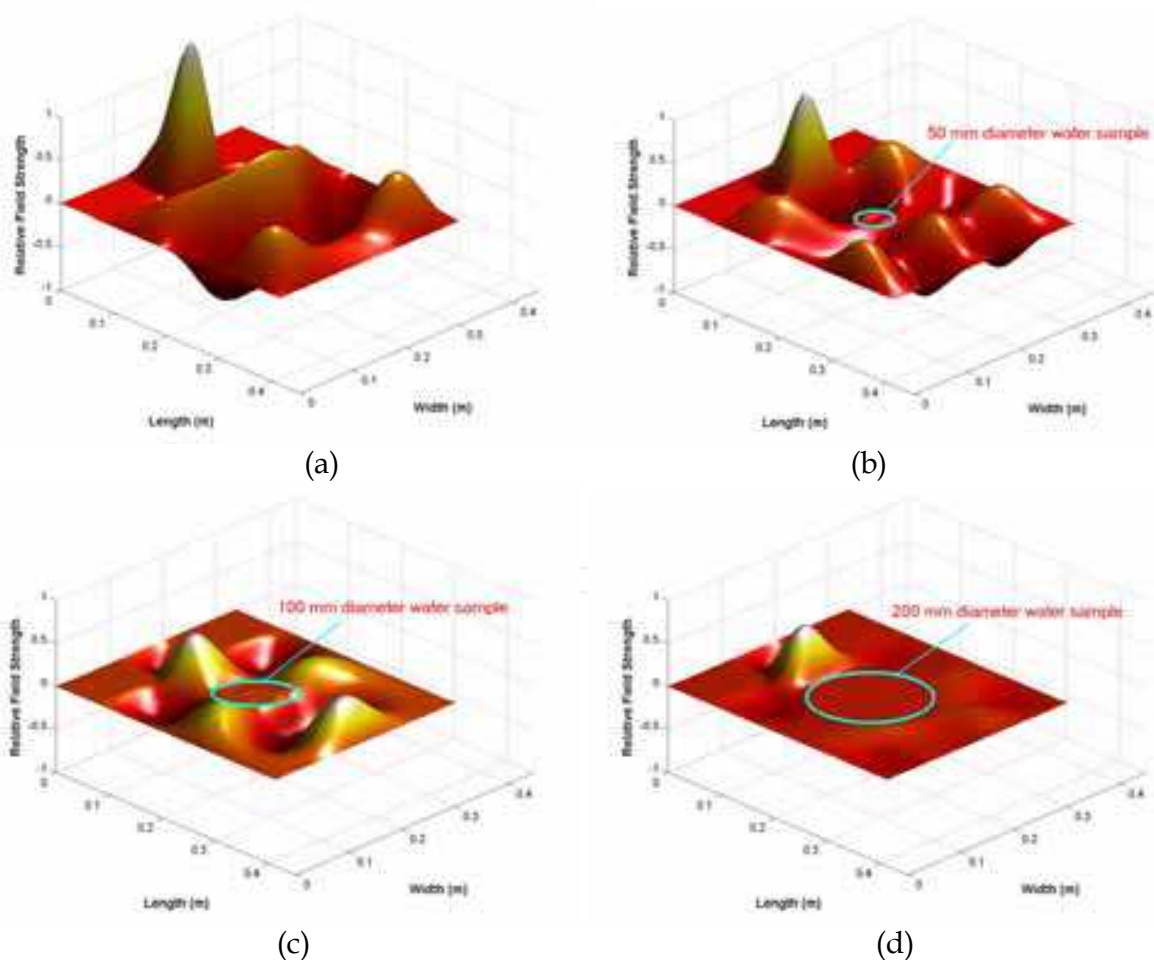


Fig. 15. FDTD simulations of the microwave fields inside a domestic microwave oven with various sized water loads (a) empty cavity, (b) a small water load, (c) a medium sized water load and (d) a large water load

(Q) of the field resonance inside the chamber and effectively dampens the wave resonance. This field damping will affect the microwave heating time needed for a sample to reach a desired temperature. Consequently, small samples will heat much faster per unit volume than larger samples.

Similarly, when the FDTD technique is applied to a domestic oven cavity in which a disk of wood with varying moisture content is placed, it becomes apparent that as the moisture content reduces, the microwave field amplitude inside the wood sample increases (Fig. 16). This supports the earlier discussion about wave resonance inside the heated material that may lead to thermal runaway.

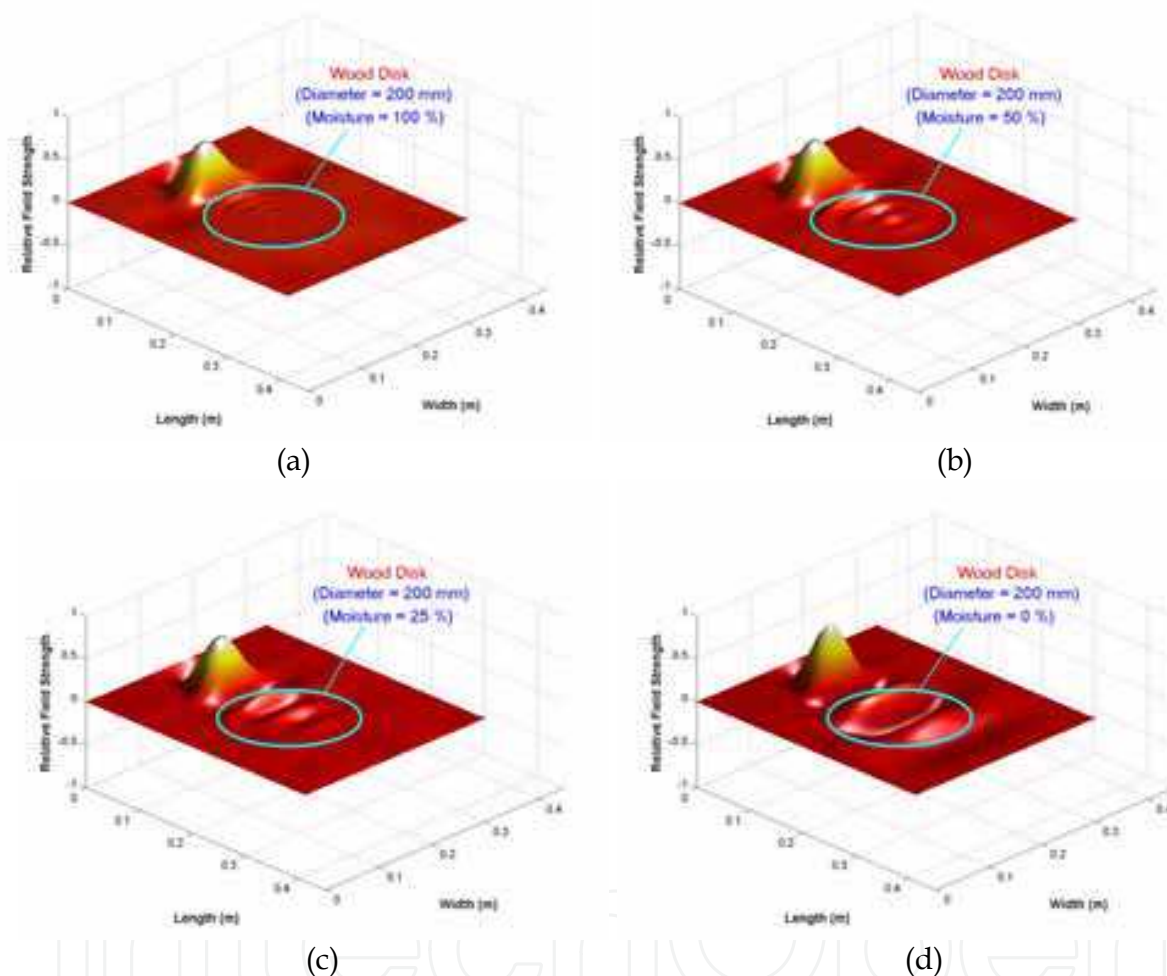


Fig. 16. FDTD simulations of the microwave fields inside a domestic microwave oven with a wooden disk of varying moisture content, measured as a percentage of oven dried wood.

5.2 Problems with the FDTD method

If aliasing of the final solution is to be avoided (Vandoren, 1982), the grid size must be small enough so that the electromagnetic field does not change significantly from one grid cell to the next. Similarly the time steps for each computational cycle must satisfy the Courant stability criterion (Yee, 1966; Taflove, 1988; Walker, 2001). This implies that the simulated time step for many problems may be no more than a few picoseconds. Therefore solving heating problems that may span many seconds or minutes of real time requires a significant number of computational iterations.

For computational stability to be satisfied (Yee, 1966; Walker, 2001), the time step used in the program must satisfy:

$$\Delta t \leq \frac{\sqrt{(\Delta x)^2 + (\Delta y)^2 + (\Delta z)^2}}{c} \quad (66)$$

When establishing an appropriate grid for analysis, it must be remembered that the wavelength of the microwaves inside a dielectric material is:

$$\lambda = \frac{\lambda_0}{\sqrt{\kappa'}} \quad (67)$$

The values of Δx , Δy and Δz must be small compared to λ to ensure accurate simulations. Since FDTD requires that the entire computational domain be gridded, and these grids must be small compared to the smallest wavelength and smaller than the smallest feature in the model, very large computational domains can be developed. This implies that very long calculation times are needed to simulate real microwave heating systems.

To put this into perspective, simulating the first 20 nanoseconds of electromagnetic activity inside a 335 mm by 335 mm by 205 mm microwave oven that has a cup (cylinder) of water in it, using a 4 mm grid, requires approximately 30 minutes of uninterrupted computational time on a Pentium 4 computer. Trying to simulate 10 minutes of real time would take 950 years on the same machine using the same code.

FDTD finds the E/H fields everywhere in the computational domain. If the field values at some distance from the microwave source (like 10 meters away) are required, the computational domain will be excessively large. Far field extensions, which apply a Fast Fourier Transformation to the field distribution in a fixed plane of the FDTD computational domain are available, but this usually requires some post processing rather than direct calculations.

Most authors use FDTD and other numerical techniques to analyse “static systems”. This implies that apart from the initial field excitation imposed onto the system, all other components are stationary. Commercial microwave applicators use mode stirrers (Metaxas & Meredith, 1983) or movement of the heated product relative to the microwave fields to deliberately perturb the fields and more evenly irradiate the load. Consequently, any attempt to evaluate the electric field, including numerical techniques, only provides an approximation of the field strength (Kopyt et al., 2003).

6. Applications of microwave heating

Throughout this discussion various applications of microwave heating have been mentioned. Microwave heating is now a standard method in food preparation and in some industrial processes (Metaxas & Meredith, 1983). In industry, microwave heating is used for drying of wood (Zielonka & Dolowy, 1998; Antti & Perre, 1999), paper and cardboard (Hasna et al., 2000), textiles, and leather (Ayappa et al., 1991). Other uses include oil extraction from tar sands, cross-linking of polymers, metal casting (Ayappa et al., 1991), medical applications (Bond et al., 2003), pest control (Nelson & Stetson, 1974; Nelson, 1996), enhancing seed germination (Nelson et al., 1976; Nelson & Stetson, 1985), and solvent-free chemistry (Arrieta et al., 2007).

More recently, microwave heating has been used to modify the structure of wood (Vinden & Torgovnikov, 2000; Torgovnikov & Vinden, 2005) allowing it to dry much faster (Brodie, 2007a) and be impregnated with resins to make it stronger (Przewloka et al., 2007). Microwave energy has also been used to manage weeds and other soil born pathogens (Nelson, 1987; Bansal, 2006) and to treat various animal feeds to improve their digestibility (Sadeghi & Shawrang, 2006, 2007; Brodie et al., 2010). Microwaves are commonly used to process ceramics (Takayama et al., 2005) and can be used to drill through ceramics and glass (Jerby et al., 2002).

7. Conclusion

The major advantages of microwave heating are its short startup, precise control, and volumetric heating (Ayappa et al., 1991); however non-uniform heating, rapid drying and unstable temperatures are commonly reported. This chapter has explored some of the reasons why these three features of microwave heating occur. Mathematical models and simulation techniques reveal that object geometry, size, moisture content, dielectric properties, and heating time all profoundly affect temperature/moisture distributions during microwave heating. Small slabs, cylinders, and spheres, with low dielectric loss, exhibit pronounced core heating, while increasing the size of the object or the dielectric loss of the material results in pronounced subsurface heating.

8. Nomenclature

Ω	= combined temperature and moisture vapour parameter
Ω_0	= Initial condition of the combined temperature and moisture vapour parameter
a_w	= air space fraction in the material
c	= speed on light (m s^{-1})
C	= thermal capacity of the composite material ($\text{J kg}^{-1} \text{ }^\circ\text{C}^{-1}$)
D_a	= vapor diffusion coefficient of water vapor in air ($\text{m}^2 \text{ s}^{-1}$)
E	= electric field associated with the microwave (V m^{-1})
E_0	= magnitude of the electric field external to the work load (V m^{-1})
f	= complex wave number of the form $f = \alpha + j\beta$
h	= convective heat transfer at the surface of a heated object ($\text{W m}^{-1} \text{ K}^{-1}$)
H	= magnetic field associated with the microwave
$i_0(x)$	= modified spherical Bessel function of the first kind of order zero
$I_0(z)$	= modified Bessel function of the first kind of order zero
j	= complex operator $\sqrt{-1}$
\mathcal{J}	= current flux due to internal conduction
$j_0(x)$	= spherical Bessel function of the first kind of order zero
$\mathcal{J}(z)$	= Bessel function of the first kind of order zero
\mathcal{J}	= current sources that may be embedded within the region of interest
k	= thermal conductivity of the composite material ($\text{W m}^{-1} \text{ }^\circ\text{C}^{-1}$)
$K_0(z)$	= modified Bessel function of the second kind of order zero
L	= latent heat of vaporization of water (J kg^{-1})
M_s	= moisture content of the solid material (kg kg^{-1})
M_v	= moisture vapor concentration in the pores of the material (kg m^{-3})

n	= constant of association relating water vapor concentration to internal temperature of a solid
p	= constant of association relating internal temperature of a solid to water vapor concentration
q	= volumetric heat generated by microwave fields ($W\ m^{-3}$)
r	= radial distance from the centre of a cylinder or sphere (m)
r_o	= external radius of the cylinder or sphere (m)
s	= Laplace transformation argument
t	= heating time (s)
T	= temperature ($^{\circ}C$)
W	= thickness of the slab (m)
$Y_o(z)$	= Bessel function of the second kind of order zero
z	= linear distance from the surface of a slab (m)
Δt	= incremental time step (s)
Δx	= incremental distance (m)
Δy	= incremental distance (m)
Δz	= incremental distance (m)
Γ	= internal reflection coefficient
α	= real part of the complex wave number f
β	= imaginary part of the complex wave number f
χ	= concentration of agar in agar gel (%)
δ	= phase shift of microwave fields at the surface of a material
ϵ^*	= complex electrical permittivity of the space through which the waves are propagating
ϵ_s	= the dielectric properties of a material at very low frequencies
γ	= combined diffusivity for simultaneous heat and moisture transfer
κ'	= relative dielectric constant of the material
κ''	= dielectric loss factor of the material
λ	= wave length inside a material (m)
λ_o	= wave length in free space (m)
μ	= magnetic permeability of the space through which the waves are propagating
θ_A	= phase angle associated with forward propagating wave in rectangular coordinate system
θ_B	= phase angle associated with reverse propagating wave in rectangular coordinate system
ρ	= composite material density ($kg\ m^{-3}$)
ρ_c	= charge density within the space through which the waves are propagating
ρ_s	= density of the solid material ($kg\ m^{-3}$)
σ	= constant of association relating moisture vapor concentration to moisture content in a solid
σ_c	= electrical conductivity of the material ($S\ m^{-1}$)
τ	= transmission coefficient for incoming microwave
τ_v	= tortuosity factor
ω	= angular frequency ($rad\ s^{-1}$)
$\Re(z)$	= real part of the complex number z

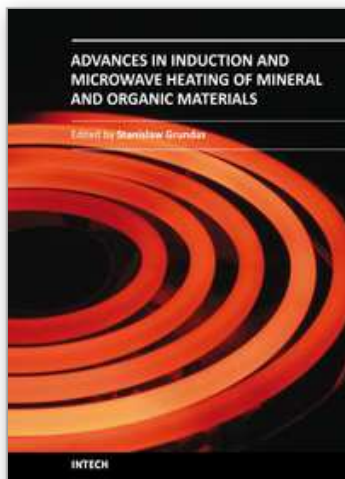
9. References

- Antti, A. L. and Perre, P. 1999. A microwave applicator for on line wood drying: Temperature and moisture distribution in wood. *Wood Science and Technology*, vol. 33, no. 2, pp. 123-138, ISSN: 0043-7719
- Arrieta, A., Otaegui, D., Zubia, A., Cossio, F. P., Diaz-Ortiz, A., delaHoz, A., Herrero, M. A., Prieto, P., Foces-Foces, C., Pizarro, J. L. and Arriortua, M. I. 2007. Solvent-Free Thermal and Microwave-Assisted [3 + 2] Cycloadditions between Stabilized Azomethine Ylides and Nitrostyrenes. An Experimental and Theoretical Study. *Journal of Organic Chemistry*, vol. 72, no. 12, pp. 4313-4322, ISSN: 0022-3263
- Ayappa, K. G., Davis, H. T., Crapiste, G., Davis, E. J. and Gordon, J. 1991. Microwave heating: An evaluation of power formulations. *Chemical Engineering Science*, vol. 46, no. 4, pp. 1005-1016, ISSN: 0009-2509
- Bansal, R. 2006. Microwave surfing: yard work [Agricultural machinery]. *Microwave Magazine, IEEE*, vol. 7, no. 4, pp. 26-28, ISSN: 1527-3342
- Bond, E. J., Li, X., Hagness, S. C. and Van Veen, B. D. 2003. Microwave imaging via space-time beamforming for early detection of breast cancer. *IEEE Transaction on Antennas and Propagation*, vol. 51, no. 8, pp. 1690-1705, ISSN: 0018-926X
- Bowman, F. 1931, *Elementary Calculus*, Longmans, Green and Co. Ltd., ISBN: 0582318076, London.
- Brodie, G. 2005. Microwave preconditioning to accelerate solar drying of timber, In: *Microwave and Radio Frequency Applications: Proceedings of the Fourth World Congress on Microwave and Radio Frequency Applications*, Schulz, R. L. and Folz, D. C. (Eds), pp. 41-48, The Microwave Working Group, ISBN: 0 97862222 0 0, Arnold MD
- Brodie, G. 2007a. Microwave treatment accelerates solar timber drying. *Transactions of the American Society of Agricultural and Biological Engineers*, vol. 50, no. 2, pp. 389-396, ISSN: 2151-0032
- Brodie, G. 2007b. Simultaneous heat and moisture diffusion during microwave heating of moist wood. *Applied Engineering in Agriculture*, vol. 23, no. 2, pp. 179-187, ISSN: 0883-8542
- Brodie, G. 2008. The Influence of Load Geometry on Temperature Distribution During Microwave Heating. *Transactions of the American Society of Agricultural and Biological Engineers*, vol. 51, no. 4, pp. 1401-1413, ISSN: 2151-0032
- Brodie, G., Rath, C., Devanny, M., Reeve, J., Lancaster, C., Harris, G., Chaplin, S. and Laird, C. 2010. The effect of microwave treatment on lucerne fodder. *Animal Production Science*, vol. 50, no. 2, pp. 124-129, ISSN: 1836-0939
- Chu, J. L. and Lee, S. 1993. Hygrothermal stresses in a solid: Constant surface stress. *Journal of Applied Physics*, vol. 74, no. 1, pp. 171-188, ISSN: 0021-8979
- Crank, J. 1979, *The Mathematics of Diffusion*, J. W. Arrowsmith Ltd., ISBN: 0-19-853411-6, Bristol.
- El-Rayes, M. A. and Ulaby, F. T. 1987. Microwave Dielectric Spectrum of Vegetation-Part I: Experimental Observations. *IEEE Transactions on Geoscience and Remote Sensing*, vol. GE-25, no. 5, pp. 541 - 549 ISSN: 0196-2892
- Fan, J., Luo, Z. and Li, Y. 2000. Heat and moisture transfer with sorption and condensation in porous clothing assemblies and numerical simulation. *International Journal of Heat and Mass Transfer*, vol. 43, no. 16, pp. 2989-3000, ISSN: 0017-9310

- Fan, J., Cheng, X., Wen, X., and Sun, W. 2004. An improved model of heat and moisture transfer with phase change and mobile condensates in fibrous insulation and comparison with experimental results. *International Journal of Heat and Mass Transfer*, vol. 47, no. 10-11, pp. 2343-2352, ISSN: 0017-9310
- Hasna, A., Taube, A. and Siores, E. 2000. Moisture Monitoring of Corrugated Board During Microwave Processing. *Journal of Electromagnetic Waves and Applications*, vol. 14, no. 11, p. 1563, ISSN: 0920-5071
- Henry, P. S. H. 1948. The diffusion of moisture and heat through textiles. *Discussions of the Faraday Society*, vol. 3, pp. 243-257, ISSN: 0366-9033
- Hill, J. M. and Marchant, T. R. 1996. Modelling Microwave Heating. *Applied Mathematical Modeling*, vol. 20, no. 1, pp. 3-15, ISSN: 0307-904X
- Jerby, E., Dikhtyar, V., Aktushev, O. and Groszlick, U. 2002. The microwave drill. *Science*, vol. 298, no. 5593, pp. 587-589, ISSN: 0193-4511
- Kopyt, P., Celuch-Marcysiak, M. and Gwarek, W. K. 2003. Microwave processing of temperature-dependent and rotating objects: Development and experimental verification of FDTD algorithms, In: *Microwave and Radio Frequency Applications: Proceeding of the Third World Congress on Microwave and Radio Frequency Applications*, Folz, D. C., Booske, J. H., Clark, D. E. and Gerling, J. F. (Eds), pp. 7-16, The American Ceramic Society, ISBN: 1 57498 158 7, Westerville, Ohio
- Kritikos, H. N., Foster, K. R. and Schwan, H. P. 1981. Temperature profiles in spheres due to electromagnetic heating. *Journal of Microwave Power and Electromagnetic Energy*, vol. 16, no. 3 and 4, pp. 327-340, ISSN: 0832-7823
- Lawrence, A. 2006. Effect of microwave modification on the density of eucalyptus obliqua wood. *Journal of the Timber Development Association of India*, vol. 52, no. 1/2, pp. 26-31, ISSN: 0377-936X
- Liu, B. and Marchant, T. R. 2002. The microwave heating of three-dimensional blocks: semi-analytical solutions. *IMA Journal of Applied Mathematics*, vol. 67, no. 2, pp. 145 -175, ISSN: 1110-757X
- Meredith, R. J. 1994. A three axis model of the mode structure of multimode cavities. *The Journal of Microwave Power and Electromagnetic Energy*, vol. 29, no. 1, pp. 31-44, ISSN: 0832-7823
- Metaxas, A. C. and Meredith, R. J. 1983, *Industrial Microwave Heating*, Peter Peregrinus, ISBN: 0 906048 89 3, London.
- Murray, D. 1958. Percy Spencer and his itch to know. *Reader's Digest*, vol. August, ISSN: 0034-0413
- Nelson, M. I., Wake, G. C., Chen, X. D. and Balakrishnan, E. 2001. The multiplicity of steady-state solutions arising from microwave heating. I. Infinite Biot number and small penetration depth. *The ANZIAM Journal*, vol. 43, no. 1, pp. 87-103, ISSN: 1446-1811
- Nelson, S. O. 1987. Potential agricultural applications of RF and microwave energy. *Transactions of the ASAE*, vol. 30, no. 3, pp. 818-831, ISSN: 0001-2351
- Nelson, S. O. 1996. Review and assessment of radio-frequency and microwave energy for stored-grain insect control. *Transactions of the ASAE*, vol. 39, no. 4, pp. 1475-1484, ISSN: 0001-2351
- Nelson, S. O. and Stetson, L. E. 1974. Possibilities for Controlling Insects with Microwaves and Lower Frequency RF Energy. *IEEE Transactions on Microwave Theory and Techniques*, vol. December 1974, pp. 1303-1305, ISSN: 0018-9480

- Nelson, S. O. and Stetson, L. E. 1985. Germination responses of selected plant species to RF electrical seed treatment. *Transactions of the ASAE*, vol. 28, no. 6, pp. 2051-2058, ISSN: 0001-2351
- Nelson, S. O., Ballard, L. A. T., Stetson, L. E. and Buchwald, T. 1976. Increasing legume seed-germination by VHF and microwave dielectric heating. *Transactions of the ASAE*, vol. 19, no. 2, pp. 369-371, ISSN: 0001-2351
- Ohlsson, T. and Risman, P. O. 1978. Temperature distributions of microwave heating - spheres and cylinders. *Journal of Microwave Power and Electromagnetic Energy*, vol. 13, no. 4, pp. 303-310, ISSN: 0832-7823
- Oliveira, M. E. C. and Franca, A. S. 2002. Microwave heating of foodstuffs. *Journal of Food Engineering*, vol. 53, no. 4, pp. 347-359, ISSN: 0260-8774
- Przewloka, S. R., Hann, J. A. and Vinden, P. 2007. Assessment of commercial low viscosity resins as binders in the wood composite material Vintorg. *Holz als Roh - und Werkstoff*, vol. 65, no. 3, pp. 209-214, ISSN: 0018-3768
- Romano, V. R., Marra, F. and Tammaro, U. 2005. Modelling of microwave heating of foodstuff: study on the influence of sample dimensions with a FEM approach. *Journal of Food Engineering*, vol. 71, no. 3, pp. 233-241, ISSN: 0260-8774
- Sadeghi, A. A. and Shawrang, P. 2006. Effects of microwave irradiation on ruminal protein and starch degradation of corn grain. *Animal Feed Science and Technology*, vol. 127, no. 1-2, pp. 113-123, ISSN: 0377-8401
- Sadeghi, A. A. and Shawrang, P. 2007. Effects of microwave irradiation on ruminal protein degradation and intestinal digestibility of cottonseed meal. *Livestock Science*, vol. 106, no. 2-3, pp. 176-181, ISSN: 1871-1413
- Shaw, T. M. and Galvin, J. A. 1949. High-Frequency-Heating Characteristics of Vegetable Tissues Determined from Electrical-Conductivity Measurements. *Proceedings of the IRE*, vol. 37, no. 1, pp. 83-86, ISSN: 0096-8390
- Taflove, A. 1988. Review of the formulation and applications of the finite-difference time-domain method for numerical modeling of electromagnetic wave interactions with arbitrary structures. *Wave Motion*, vol. 10, no. 6, pp. 547-582, ISSN: 0165-2125
- Takayama, S., Link, G., Sato, M. and Thumm, M. 2005. Microwave sintering of metal powder compacts, In: *Microwave and Radio Frequency Applications: Proceedings of the Fourth World Congress on Microwave and Radio Frequency Applications*, Schulz, R. L. and Folz, D. C. (Eds), pp. 311-318, The Microwave Working Group, ISBN: 0 97862222 0 0, Arnold MD
- Torgovnikov, G. and Vinden, P. 2003. Innovative microwave technology for the timber industry, In: *Microwave and Radio Frequency Applications: Proceedings of the Third World Congress on Microwave and Radio Frequency Applications*, Folz, D. C., Booske, J. H., Clark, D. E. and Gerling, J. F. (Eds), pp. 349-356, The American Ceramic Society, ISBN: 1-57498-158-7, Westerville, Ohio
- Torgovnikov, G. and Vinden, P. 2005. New microwave technology and equipment for wood modification, In: *Microwave and Radio Frequency Applications: Proceedings of the Fourth World Congress on Microwave and Radio Frequency Applications*, Schulz, R. L. and Folz, D. C. (Eds), pp. 91-98, The Microwave Working Group, ISBN: 0 97862222 0 0, Arnold MD
- Van Remmen, H. H. J., Ponne, C. T., Nijhuis, H. H., Bartels, P. V. and Herkhof, P. J. A. M. 1996. Microwave Heating Distribution in Slabs, Spheres and Cylinders with

- Relation to Food Processing. *Journal of Food Science*, vol. 61, no. 6, pp. 1105-1113, ISSN: 0022-1147
- Vandoren, A. 1982, *Data Acquisition Systems*, Reston Publishing, ISBN: 0835912167, Reston, Virginia.
- Vos, M., Ashton, G., Van Bogart, J. and Ensminger, R. 1994. Heat and Moisture Diffusion in Magnetic Tape Packs. *IEEE Transactions on Magnetics*, vol. 30, no. 2, pp. 237-242, ISSN: 0018-9464
- Vriezinga, C. A. 1996. Thermal runaway and bistability in microwave heated isothermal slabs. *Journal of Applied Physics*, vol. 79, no. 3, pp. 1779 -1783, ISSN: 0021-8979
- Vriezinga, C. A. 1998. Thermal runaway in microwave heated isothermal slabs, cylinders, and spheres. *Journal of Applied Physics*, vol. 83, no. 1, pp. 438 -442, ISSN: 0021-8979
- Vriezinga, C. A. 1999. Thermal profiles and thermal runaway in microwave heated slabs. *Journal of Applied Physics*, vol. 85, no. 7, pp. 3774 -3779, ISSN: 0021-8979
- Vriezinga, C. A., Sanchez-Pedreno, S. and Grasman, J. 2002. Thermal runaway in microwave heating: a mathematical analysis. *Applied Mathematical Modelling*, vol. 26, no. 11, pp. 1029 -1038, ISSN: 0307-904X
- Wang, Z., Li, Y., Kowk, Y. L. and Yeung, C. Y. 2002. Mathematical simulation of the perception of fabric thermal and moisture sensation. *Textile Research Journal*, vol. 72, no. 4, pp. 327-334, ISSN: 0040-5175
- XiMing, W., ZhengHua, X., LiHui, S. and WeiHua, Z. 2002. Preliminary study on microwave modified wood. *China Wood Industry Journal*, vol. 16, no. 4, pp. 16-19, ISSN: 1001-8654
- Yee, K. S. 1966. Numerical solution of initial boundary value problems involving Maxwell's equations in isotropic media. *IEEE Transactions on Antennas and Propagation*, vol. 14, no. 3, pp. 302-307, ISSN: 0018-926X
- Youngman, M. J., Kulasiri, D., Woodhead, I. M. and Buchan, G. D. 1999. Use of a combined constant rate and diffusion model to simulate kiln-drying of Pinus radiata Timber. *Silva Fennica*, vol. 33, no. 4, pp. 317-325, ISSN: 0037-5330
- Yousif, H. A. and Melka, R. 1997. Bessel function of the first kind with complex argument. *Computer Physics Communications*, vol. 106, no. 3, pp. 199-206, ISSN: 0010-4655
- Zielonka, P. and Dolowy, K. 1998. Microwave Drying of Spruce: Moisture Content, Temperature and Heat Energy Distribution. *Forest Products Journal*, vol. 48, no. 6, pp. 77-80, ISSN: 0015-7473
- Zielonka, P. and Gierlik, E. 1999. Temperature distribution during conventional and microwave wood heating. *Holz als Roh- und Werkstoff*, vol. 57, no. 4, pp. 247-249, ISSN: 0018-3768
- Zielonka, P., Gierlik, G., Matejak, M. and Dolowy, K. 1997. The comparison of experimental and theoretical temperature distribution during microwave wood heating. *Holz als Roh- und Werkstoff*, vol. 55, no. 6, pp. 395-398, ISSN: 0018-3768



Advances in Induction and Microwave Heating of Mineral and Organic Materials

Edited by Prof. Stanisław Grudas

ISBN 978-953-307-522-8

Hard cover, 752 pages

Publisher InTech

Published online 14, February, 2011

Published in print edition February, 2011

The book offers comprehensive coverage of the broad range of scientific knowledge in the fields of advances in induction and microwave heating of mineral and organic materials. Beginning with industry application in many areas of practical application to mineral materials and ending with raw materials of agriculture origin the authors, specialists in different scientific area, present their results in the two sections: Section 1-Induction and Microwave Heating of Mineral Materials, and Section 2-Microwave Heating of Organic Materials.

How to reference

In order to correctly reference this scholarly work, feel free to copy and paste the following:

Graham Brodie (2011). Microwave Heating in Moist Materials, *Advances in Induction and Microwave Heating of Mineral and Organic Materials*, Prof. Stanisław Grudas (Ed.), ISBN: 978-953-307-522-8, InTech, Available from: <http://www.intechopen.com/books/advances-in-induction-and-microwave-heating-of-mineral-and-organic-materials/microwave-heating-in-moist-materials>

INTECH
open science | open minds

InTech Europe

University Campus STeP Ri
Slavka Krautzeka 83/A
51000 Rijeka, Croatia
Phone: +385 (51) 770 447
Fax: +385 (51) 686 166
www.intechopen.com

InTech China

Unit 405, Office Block, Hotel Equatorial Shanghai
No.65, Yan An Road (West), Shanghai, 200040, China
中国上海市延安西路65号上海国际贵都大饭店办公楼405单元
Phone: +86-21-62489820
Fax: +86-21-62489821

© 2011 The Author(s). Licensee IntechOpen. This chapter is distributed under the terms of the [Creative Commons Attribution-NonCommercial-ShareAlike-3.0 License](#), which permits use, distribution and reproduction for non-commercial purposes, provided the original is properly cited and derivative works building on this content are distributed under the same license.

IntechOpen

IntechOpen